Title
Stretch Evoked Mechanotransduction in Somatosensory Neurons and Smooth Muscle Cells

Author
Chase, Martha Ruth

Publication Date
2007-12-10

Peer reviewed|Thesis/dissertation

Stretch Evoked Mechanotransduction in Somatosensory Neurons and Smooth Muscle Cells

by

Martha Ruth Chase

DISSERTATION

Submitted in partial satisfaction of the requirements for the degree of

DOCTOR OF PHILOSOPHY

in

Cell Biology

in the

GRADUATE DIVISION

of the

Abstract

Stretch Evoked Mechanotransduction in Somatosensory Neurons and Smooth Muscle Cells

Martha Ruth Chase

The ability to sense force is critical for virtually all systems of the human body, including the cardiovascular, respiratory, and digestive systems as well as the sensory systems of touch and hearing. The identity of the protein(s) converting physical stimuli to electrical impulse generation and cellular behavior is unknown in mammals. In order to identify molecules involved in mechanotransduction, it is necessary to develop high-throughput methods to assess the function of many genes at once. We have addressed this issue by employing a stretch stimulus in conjunction with real-time calcium imaging and are now able to view responses of hundreds of cells simultaneously. Using this system, we have uncovered the basic principles of stretch-activated channel activity in both sensory neurons of the trigeminal and dorsal root ganglia and in vascular smooth muscle cells. We find that in all of these cell types, a pulse of stretch results in a fast rise in intracellular calcium that decays exponentially after release of stretch. By removing calcium outside these cells, we demonstrate that responses in neurons and in smooth muscle cells are derived from extracellular calcium entry, implying the activity of stretch-activated ion channels. Pharmacological tools were used to further describe the

characteristics of this calcium influx and to uncover differences between neuronal and vascular mechanotransduction.

Using our knowledge of response properties in these cells, we exploited the stretch technique to design two expression cloning screens for neuronal cDNAs mediating stretch sensitivity. Furthermore, we screened novel spider, scorpion, and cone snail venoms for novel peptides that could inhibit stretch responses in smooth muscle cells. The ability to monitor many cells at once enables these and many other types of loss- and gain-of-function screens that were not possible in the past. This stretch assay will accelerate both the characterization of other mechanosensitive cell types and the discovery of molecules responsible for mechanotransduction in mammals.

Dedication

I would like to first thank my advisor, David Julius, for allowing me to explore a scientific question outside of the lab's prior focus and for encouraging me to jump off experimental cliffs if the result would be worth the effort. In my six years in the lab I have never become bored with the question I pursued, and this is because David encourages his lab to ask the hard, important questions. I am also extremely grateful to the former and current members of the Julius lab for all of their advice, both scientific and personal, that has enabled me to get to this point. It has been truly motivating to be surrounded by such intelligent people. I'd like to thank Ellen Lumpkin for her input and guidance on my project. Ellen's expertise in the field of mechanosensation made a world of difference in the design of my experiments.

My support network outside the lab, including friends from UCSF and my Impala Racing Team teammates, helped me keep my life in perspective. My running partners have listened to me vent about experiments on countless mornings, and somehow they still want to meet me at 7am the next week!

I want to thank my parents, Barbara and Dale, for always asking questions and trying to understand my research. They have been pillars of support throughout my life and my biggest cheerleaders, and they always reassure me when I doubt myself.

Finally, I want to thank my husband Deepta for his patience as he relived graduate school all over again through me. (Sorry!!) His love, support, and understanding have kept me afloat so many times when I felt I was sinking. I couldn't ask for a better life companion.

Table of Contents

List of Figures

CHAPTER ONE

INTRODUCTION

The Role of Mechanotransduction in Physiology

Living things from bacteria to humans must be able to sense the physical nature of their environment. The detection of force or pressure can affect a myriad of processes and change the decisions made by a cell or an entire organism. This detection process, called mechanosensation or mechanotransduction, underlies virtually every organ system in our bodies: our blood vessels respond to changes in blood pressure, our stomach expands to accommodate food, our bladder alerts us to its filling status, and our skin senses gentle touch and painful pressure through mechanotransduction. Signals generated by mechanotransduction events alter the development of epithelial cells in the lung, endothelial cells in the vasculature, and osteoblasts in bone (Mikuni-Takagaki 1999; Waters et al. 2002; Li et al. 2005). Furthermore, in situations of inflammation or injury, mechanical stimuli that are normally benign can become noxious. Mechanosensation is fundamental to our physiology, yet we know surprisingly little about the molecular mechanisms involved in the initial detection of force by any cell type.

It is likely that most, if not all, cells are mechanosensitive to some extent. Mechanosensation in bacteria keeps these organisms alive under conditions of osmotic stress, when cells swell enough to reach lytic pressures. In humans, all cells are subjected to forces during cell division, through cell-cell contacts, and by fluid movements in the body. The ability to detect and respond to these forces to maintain cell homeostasis is likely built into every cell. On top of these ubiquitous detection processes, mechanosensation plays an even broader physiological role in the circulatory, digestive, and sensory systems, among others. Forces in these locations are critical for survival of

the organism. Cells may have varying thresholds for sensing mechanical forces depending on their physiological role.

Sensing forces can result in both constructive and detrimental cellular changes. For example, mechanical forces in the lung upon the initiation of breathing in a newborn are essential for the proper differentiation of alveolar cell types (Joe et al. 1997). In contrast, turbulent blood flow occurring at artery branch points causes shear stress which can lead to the development of atherosclerotic plaques in these locations (Birukov et al. 1995). Understanding the mechanisms contributing to sensing forces, setting mechanical thresholds, and initiating downstream effects on cells will inform many branches of medicine.

The Molecular Basis of Mechanotransduction

Numerous mechanisms have been proposed to underlie mechanotransduction. One model suggests that a diffusible factor released by stimulated cells activates receptors on nearby cells. Evidence for this model comes primarily from studies of the bladder, where ATP release from stretched endothelial cells opens the ATP gated ion channel P2X3 on visceral afferents (Cockayne et al. 2000; Vlaskovska et al. 2001). Alternatively, tension on integrins by the extracellular matrix can cause structural deformations in the actin cytoskeleton and activate downstream signaling events in many cell types (Katsumi et al. 2004). However, in cells requiring fast responses on the order of microseconds, such as inner ear hair cells and somatosensory neurons, mechanosensitive ion channels are likely activated, producing currents that cause depolarization and action potential firing.

The first mechanosensitive ion channel identified, MscL, was cloned from the bacteria *Escherichia coli* using a biochemical approach in which membrane proteins were reconstituted into liposomes and assayed for activity using suction (Sukharev et al. 1994). When reconstituted, the MscL channel is opened at pressures of ~100mmHg and has a conductance of 3 pS (Sukharev et al. 1994), values suggesting that the function of this channel is to open in conditions of potentially lytic pressures. Notably, the preservation of MscL activity in the absence of other proteins confirms that tension in the lipid bilayer is sufficient to gate the channel. Since the discovery of MscL, additional bacterial and fungal mechanosensitive channels have been identified, all of which can be gated by bilayer tension (Anishkin et al. 2005).

In multicellular organisms, the gating mechanisms appear to be more complex than in bacteria. While some channels can be opened by amphipathic molecules that cause curvature of the cell membrane (Maingret et al. 1999), others need additional proteins for gating. The most complete studies to date on mechanosensory mechanisms have come from a mutagenic screen for nose-touch deficient mutants in the nematode *Caenorhabditis elegans* (Chalfie et al. 1989). Seven transduction-related genes were identified in this screen, including three subunits of an ion channel related to the epithelial sodium channel (ENaC) family. Subsequent work demonstrated that these subunits are capable of forming a functional ion channel in heterologous systems (Goodman et al. 2002). Furthermore, by recording directly from touch-sensitive neurons in wild type and mutant worms, it was confirmed that these subunits form a conduction pathway activated by mechanical stimuli (O'Hagan et al. 2005).

ENaC channels are broadly expressed in mammals, and mouse knockouts of the ENaC family members ASIC1, ASIC2 (BNC1), and ASIC3 (DRASIC), have been generated. ASIC1 knockouts show an increased spiking frequency of visceral sensory afferents to mechanical stimuli but no changes in cutaneous mechanosensation (Page et al. 2004). ASIC2 deletion affects the firing rate of a subset of low-threshold rapidly adapting mechanosensors (Price et al. 2000), while ASIC3 deletion had opposing effects on light touch versus nociceptive neuron firing rate (Price et al. 2001). In none of these studies were currents from mechanosensitive channels recorded, so it is unclear whether these ASIC channels are contributing to the initial transduction event or to signal propagation in the neuron. Other ENaC channel subunits have been found in aortic baroreceptor nerve terminals which detect changes in arterial pressure, and while pharmacological data suggests the involvement of this channel family in the transduction process, evidence that this channel is the initial sensor is again lacking (Drummond et al. 2001).

In addition to the ENaC family, members of the transient receptor potential (TRP) ion channel family are proposed to detect mechanical stimuli in some contexts. The *C. elegans* TRP channel OSM-9 and the mammalian channel TRPV4 open in response to hypotonic solutions that cause tension in the cell membrane due to cell swelling. Osmotic activation of TRPV4 has been achieved in heterologous expression systems (Strotmann et al. 2000), but this has yet to be shown for OSM-9. In the fruit fly *Drosophila melanogaster*, the Nomp-C (no mechanoreceptor potential) gene, which encodes a TRP channel family member, is mutant in flies with deficiencies in bristle mechanotransduction (Walker et al. 2000). Nomp-C is also required for generating

microphonic potentials in response to hair cell bundle deflection in the zebrafish *Danio rerio* (Sidi et al. 2003). While these results makes Nomp-C an intriguing candidate for a mechanotransduction channel in flies and fish, Nomp-C homologues have not been found in the mammalian genome. A mammalian TRP channel, TRPA1, was initially proposed to be a mechanosensitive channel in vertebrate hair cells (Corey et al. 2004), but analysis of TRPA1 knockout mice revealed functional hearing and somatososensory responses (Bautista et al. 2006).

Clues to the identity of mechanotransduction channels have come from the characterization of mechanically induced currents in sensory cells. The most thoroughly characterized transduction currents are those found in saccular hair cells from the bullfrog. In these cells, deflection of the hair cell bundle towards the tallest stereocilia opens transduction channels, resulting in the detection of sound waves of particular frequencies. The mechanically evoked current in these cells is a nonselective cation conductance with a very short ~25μs delay in opening in response to deflection of the hair bundle at 28ºC (Corey et al. 1979; Corey et al. 1983). At this response speed, it is unlikely that any enzymatic steps or signal transduction events occur to produce channel opening, suggesting that the channel itself is the mechanosensitive element.

In mammalian sensory neurons, mechanosensitive currents have been recorded from dissociated neurons using stimuli such as suction on the cell membrane or poking with a polished pipette. These currents are nonselective cation currents, similar to those in hair cells (McCarter et al. 1999; Cho et al. 2002). Evidence suggests multiple channel types with varying thresholds exist in sensory neurons (Cho et al. 2002; Cho et al. 2006). However, the identities of these channels remain unknown.

Irrespective of channel identity, we know that in vivo, mechanical sensitivity can be altered through inflammation or injury. For example, when you get a sunburn, you can experience normally innocuous touch as painful, a process called allodynia, and you may also feel heightened responses to normally painful stimuli, called hyperalgesia. These two phenomena occur in response to temperature stimulation as well, a system that is better understood than mechanosensation. To cause thermal hyperalgesia and allodynia, inflammatory mediators bind to their receptors, activating intracellular signaling that modifies the activity of the thermosensitive TRP channel TRPV1 (Chuang et al. 2001). This modification seems to occur through both phosphorylation and through lipid interactions (Chuang et al. 2001; Vellani et al. 2001; Prescott et al. 2003). Although similar experimental inflammatory stimuli can induce both thermal and mechanical allodynia in animals, we do not understand how cells are sensitized or whether peripheral and/or central sensitization contributes to this behavior.

Technical Challenges in the Study of Mechanosenation

Electrophysiological approaches to the study of mechanotransduction provide detailed information about the nature of the ion channel, but due to their cell-by-cell nature they have limited ability to describe diversity in heterogeneous cell populations. Peripheral somatosensory neurons, with cell bodies in the dorsal root ganglion (DRG) and trigeminal ganglion (TG), include many distinct cell populations with specialized sensory endings to detect various features of touch, such as texture, vibration, and direct pressure. A higher throughput method to detect mechanosensitive channel opening is necessary to fully describe this complex set of neurons.

Another useful technique to characterize mechanotransduction events in a more native setting is the skin-nerve preparation, in which a section of skin from the hindlimb of a mouse or rat is removed with a portion of the nerve still attached (Koltzenburg et al. 1997). Recordings made from the severed axons of individual neurons allow classification of neuron types by conduction velocity and adaptation processes. Based on skin-nerve recordings in mouse, it is thought that virtually all somatosensory neurons are mechanosensitive but that subtypes vary in their stimulus-response curves (Koltzenburg et al. 1997). While the advantage of this technique is its maintenance of the intact terminal structure and detection properties, recordings are limited to firing rates and cannot detect individual receptor potentials at the terminals or characterize their currents. Furthermore, this technique does not improve the throughput of analysis, as each recording is made from a single axon.

Sensory endings in the skin are too small to be accessible to electrophysiological techniques, and most types of endings terminate in the dermis rather than the epidermis, making them difficult to access. Dissociated sensory neurons are an adequate replacement for examining transduction processes that occur at the terminals. The trafficking of transduction molecules for heat and chemicals is rarely specific to the sensory terminals in these neurons, leaving populations of these proteins on the cell bodies (Garcia-Anoveros et al. 2001). In accordance with this observation, TRPV1 expression in DRG neurons is found in the same proportions of dissociated sensory neurons as are found to be sensitive to capsaicin in the skin-nerve preparation (Caterina et al. 1997; Stucky et al. 2004).

To facilitate large-scale, high throughput analysis of mechanotransduction, we have utilized a mechanical stimulus that stretches cells adhered to a flexible silicone membrane (Banes et al. 1985) (Figure 1). This stretch stimulus allows cells on the same membrane to feel simultaneous and identical mechanical stimulation. Furthermore, we have developed a protocol to monitor the real-time responses of these cells with calcium imaging. This stretch imaging method has revealed new populations of mechanosensitive neurons. It has the potential to facilitate large scale screening approaches to identify molecules involved in mechanotransduction in neurons and in non-neuronal cells.

Figure Legends

Figure 1. The StageFlexer system uses vacuum pressure to stretch cells radially. A, Image of the StageFlexer Jr. from the top. Vacuum is applied through a tube shown on the right. B, Components of the StageFlexer, separated for clarity. From top, screws, circular top/o-ring, silicone membrane with cells, loading post, vacuum chamber. Cells are grown on the silicone membrane that is sealed with screws over a smaller diameter post. Area surrounding the post is evacuated with negative pressure applied through the side of the chamber. C, Calibration of stretch. Fluorescent beads were adhered to a silicone membrane and stretched at varying vacuum pressures. The distance between each pair of beads was calculated, divided by the starting (unstretched) value, and multiplied by 100 to get the percent stretch. The formula shown in the inset is the linear fit of the relationship between percent stretch and applied vacuum pressure.

Figure 1.

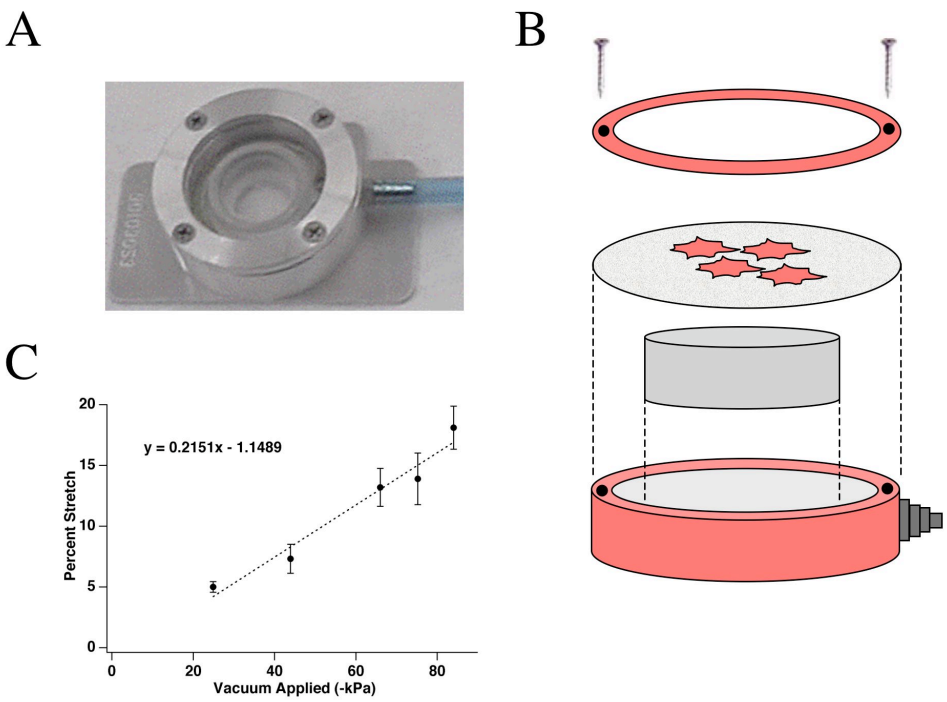
A
B
C
y = 0.2151x - 1.1489
Percent Stretch
Vacuum Applied (-kPa)
0
5
10
15
20
0
20
40
60
80

MATERIALS AND METHODS

Sensory Neuron Dissociation

All media and cell culture supplements were purchased from the UCSF Cell Culture Facility unless otherwise noted. Mice were from Charles River Laboratory, except for TrkC-EGFP mice, which were provided by Ellen Lumpkin. Neurons from neonatal trigeminal ganglia and neonatal and adult dorsal root ganglia were dissected into 1.4mg/ml Collagenase P (Roche) in Hanks Calcium-Free Balanced Salt Solution and incubated while rotating at 37ºC for 10 minutes. Neurons were pelleted at 1000rpm for 5' and incubated in 0.25% STV Trypsin for 3 minutes with gentle agitation. Complete media (MEM Eagle's with Earle's BSS medium, supplemented with 10% horse serum, vitamins, penicillin/streptomycin, and L-glutamine) was added to inactivate trypsin, and cells were pelleted at 1000rpm for 5' and resuspended in complete media. Neurons were gently triturated with a fire-polished glass pipette, pelleted, and resuspended in a small amount of complete media for plating. Trigeminal neurons were stretched after one day in culture, whereas DRG neurons required three days to be maximally stretch sensitive.

Smooth Muscle Dissociation

Aortas were removed from adult mice into phosphate-buffered saline (PBS) and the adventia and outer layer of muscle was removed with forceps. Cleaned aortas were transferred to Dulbecco's modified Eagle's Media (H-21), minced and incubated at 37ºC / 5% CO_2 for 1 hour in Solution I (1.5mg/ml Collagenase Dispase, 0.5mg/ml Elastase type IIa, 1 mg/ml Trypsin inhibitor, 2mg/ml fatty acid free BSA). Cells were then pelleted, resuspended in in Solution II (1mg/ml Collagnease Type II, 0.3mg/ml Trypsin inhibitor, 2mg/ml fatty acid free BSA), and incubated for a second hour at 37ºC / 5%

CO_2. Cells were pelleted, rinsed once with 100% Fetal Bovine Serum, pelleted and resuspended in DME H-21 with 20% FBS for the first passage. Serum was reduced to 10% in subsequent passages. Cells required approximately two weeks to assume a non-contractile, synthetic phenotype, at which point they were used for stretch experiments.

Dye Loading Procedures

For calcium imaging experiments, cells were loaded for 1 hr with 10μM Fura-2 AM (Invitrogen), supplemented with 0.02% Pluronic F-127 (Invitrogen), in a physiological ringer solution containing (in mM) 140 NaCl, 5KCl, 10 HEPES, 2 $CaCl_2$, 2$MgCl_2$, 10 D-(+)-glucose, pH 7.4. For FM 1-43 loading experiments, solutions containing 10μM FM-143 (Biotium Inc.) were used during stretch. All chemicals were purchased from Sigma.

Stretch Stimulation

Circular membranes were cut with an arch punch from sheets of glossy silicone of 0.02" thickness (Specialty Manufacturing Inc.) and coated with ~15μg/ml laminin for 2 hours (for neurons) or for 30-60 minutes with fibronectin (for muscle cells and human embryonic kidney cells). Cells were spotted in 10-25μl in the center of each membrane and allowed to adhere for 1-2 hours at 37ºC before adding the appropriate media. For smooth muscle experiments, cells received serum-free media for at least 12 hours before stretching.

Membranes were mounted onto the StageFlexer system (Flexcell International Corp.) and vacuum pressure was applied through the FX-3000 system (Flexcell). Periodic calibrations were done using fluorescent beads attached to the silicone membranes, and images of the beads were taken before and during a static stretch. To

stimulate cells, a 2 second square wave of vacuum pressure was applied (unless otherwise noted). Maximum vacuum pressure was achieved at approximately 0.4 sec after the start of the stimulus. Cells were imaged with an upright BX51WI microscope (Olympus) and illumination was achieved with a Lambda LS arc lamp and Lambda 10-3 filter wheel system (Sutter). Images were acquired at 3 second intervals with a Hamamatsu Orca ER digital camera controlled by MetaFluor v 7.0 software (Molecular Devices).

For FM1-43 loading experiments, cells were incubated with 10μM FM 1-43 (Biotium Inc.) for 90 seconds and stretched 3 times for 2 seconds each during the incubation. Cells were immediately washed with 500mM Advasep-7 (Biotium) followed by Ringer's solution and examined with fluorescence microscopy.

Data Analysis

Acquired images were displayed as the ratio of the 340nm to 380nm image, background subtracted based on a zero calcium calibration (see below), and saved. Images were aligned in MetaMorph using a custom-designed alignment macro. Regions were drawn and data saved in MetaMorph. Traces were analyzed in Igor Pro (WaveMetrics) using custom designed programs. The first frame in focus after stretch often contained a stimulus artifact and was excluded from analysis. A responder was defined using three criteria: 1) a response larger than 5 times the standard deviation of the pre-stretch calcium level at the start of the experiments, 2) at least 3 points above the calcium level immediately preceding the stretch, and 3) an exponentially recovering or otherwise quickly recovering response (no plateau). Neurons were identified by treatment with high potassium solution (75mM) at the end of each experiment.

Venom Screening

Small chambers holding 30-50µl of solution were constructed on membranes using a syringe filled with non-toxic silicone sealant (DAP Incorprated, Center Hardware, San Francisco) and allowed to dry. Cells plated in these chambers were serum depleted overnight before experiments. Initial venom screening was done by stretching first in the absence of toxin, waiting 10 minutes, applying venom at 1:100 dilution for 5 minutes, and stretching in the presence of venom. Ionomycin was used to control for venom effects on general calcium handling in cells. Venoms causing significant block were repeated in single stretch experiments (venom and control done on different cells). The dose response was constructed from these single stretch experiments.

Experiments testing activation of cells by venoms were done in chambered coverglass wells on a BX51WI inverted microscope (Olympus).

HPLC Fractionation

Venoms were applied to a C-8 reversed phase column in water containing 0.1% trifluoroacetic acid (TFA). 5-10 µl of venom diluted up to 100µl was used per run. Gradient fractionation occurred on a HPLC (Varian ProStar) with a ramp of 0-54% acetonitrile in constant 0.1% TFA over 40 minutes at a rate of 1ml/min. Fractions were collected every 1 ml and lyophilized. Each fraction was resuspended in 2mM calcium Ringer and diluted as necessary to test for activity.

Injury Models

Wild type mice were injected with CFA (1:1 in PBS) in both hind paws or PBS alone in both hind paws. Inflammation was allowed to develop for at least 3 days, a point at which the maximum behavioral sensitivity is reached. Ganglia from the L4-L6 region

of the spinal cord were dissected as described above and cultured for three days before assaying for stretch sensitivity.

CHAPTER TWO

MECHANISMS OF VASCULAR SMOOTH MUSCLE MECHANOTRANSDUCTION

Introduction

In the circulatory system, large blood vessels regulate their diameters by sensing forces from their lumen (blood pressure) and expanding or contracting to keep the overall pressure on the vessel relatively constant, a process called the myogenic response (Hill et al. 2001). This response is designed to maintain a basal level of constriction or tone in arteries. Smooth muscle cells lining the artery walls control the vasodilation and vasoconstriction necessary to achieve this equilibrium.

Smooth muscle cells are subjected to repeated mechanical strain that is perpendicular to the blood vessel wall, and their behavior is profoundly affected by this force. Individual cells reorient their cytoskeleton over time to be almost perpendicular to the direction of cyclical mechanical strain (Hayakawa et al. 2001). Consistent mechanical stimulation increases SMC secretion of extracellular matrix proteins such as elastin (Kolpakov et al. 1995). Furthermore, in situations of abnormally high strain, such as during sustained high blood pressure, vascular smooth muscle cells show hypertrophy and hyperplasia (Ross 1993). This cellular response worsens constriction of blood vessels by thickening artery walls and reducing pliancy.

Calcium is required for the contractile response in all muscle types. In smooth muscle cells, calcium binds to caldesmon and calmodulin, and this complex initiates the contraction cycle by activating myosin light chain kinase. When calcium is removed from extracellular medium bathing intact arteries, myogenic tone is lost and contractile response is inhibited (Hynes et al. 1991). In contrast, when arteries are treated with ryanodine to deplete intracellular calcium stores in the sarcoplasmic reticulum, the myogenic response is only minimally affected (McCarron et al. 1997). Therefore,

increased plasma membrane permeability to calcium is critical for depolarizing smooth muscle and initiating contraction.

Mechanosensitive currents in smooth muscle cells have been identified and characterized; they are nonselective cation currents that increase in magnitude with the stimulus intensity (Wu et al. 2001). This current depolarizes cells and activates L-type voltage-gated calcium channels, thus enhancing the intracellular calcium concentration and amplifying the calcium-evoked contractile response. Some studies have suggested that L-type channels are the primary mechanosensor (Lyford et al. 2002), but these data suffer from lack of a specific blocker to identify the mechanosensitive current recorded. Unfortunately, we know little about the channel due to the lack of selective blocking agents in native systems.

Calcium imaging has been used to examine the spatial distribution of mechanical responses in single smooth muscle cells (Kirber et al. 2000; Zou et al. 2002). In these studies, mechanosensitive (MS) channels were opened by suction through a patch pipette while simultaneously imaging the entire cell. An initial local rise in $[Ca^{2+}]_{int}$ due to MS channel opening is followed by a global signal propagation mediated by voltage-gated ion channels. Depletion of intracellular stores with ryanodine and thapsigargin reduced the magnitude of the calcium response to focal stretch in one study(Kirber et al. 2000) but had no effect on stretch-activated channel calcium influx in the other (Zou et al. 2002). Despite this conflict on the role of calcium stores, it is clear that calcium enters through stretch activated channels and can induce depolarization and ultimately contraction.

Because of the important physiological role that mechanosensitive calcium influx plays in vascular smooth muscle cells, we chose them as a model for studying

mechanosensation in mammalian cells. It is not known whether mechanisms underlying stretch sensitivity in smooth muscle are identical to those in sensory neurons, endothelial cells, or other mechanically sensitive mammalian cell types. However, unlike sensory neurons, cultures of smooth muscle cells are homogeneous and can be propagated in vitro, allowing for easier characterization of mechanical responses.

Results

We first demonstrated that dissociated smooth muscle cells can respond to stretch on silicone membranes (Figure 2A). Using a two second pulse of stretch which extends the membrane to 116% of its resting length (hereafter referred to as a 16% stretch), we observed large increases in intracellular calcium in rat aortic smooth muscle cells that returned to baseline with a time constant (τ) of 1.6 minutes. These cells could be repeatedly activated (Figure 2B), although in order to get approximately equivalent response magnitudes, cells required a 15 minute interval between stimuli. This recovery requirement could reflect a property of the stretch-activated channel, the necessity to refill intracellular stores, or a change in cellular properties as a result of stretch (cytoskeletal rearrangement) that recovers with time. Importantly, the ability of cells to respond to multiple stimuli demonstrates that stretch responses are not due to cellular damage. Thus, stretch is able to activate increases in intracellular calcium, similar to other methods of mechanical stimulation.

A stretch-response curve was constructed from the smooth muscle stretch responses (Figure 3). Both the magnitude of the calcium response and the percent of cells which showed responsiveness increase with the strength of the stretch stimulus. In rat long-term cultured smooth muscle cells, such as those shown in Figure 1, the half-

maximal calcium response occurred at 6.6 +/- 2.1% stretch (Figure 3A). Approximately 90% of smooth muscle cells respond to a 10% stretch stimulus with increases in intracellular calcium (Figure 3C). To verify that these responses were not an artifact of this particular line of smooth muscle cells, we made primary cultures of smooth muscle cells from adult mouse aorta and tested their responses to stretch. These cells showed slightly reduced sensitivity compared to the rat SMC cell line, but their responses were qualitatively similar. Mouse primary SMCs showed half-maximal responses at 7.4 +/- 0.96% stretch (Figure 3B). In order to activate 90% of cells in these cultures, a 16% stretch stimulus was required (Figure 3D). While the increased sensitivity of passaged cells may reflect changes that occur during long-term propagation of the rat line or species-specific differences, it could also suggest increased heterogeneity in primary cultures such that cells are of a range of sensitivities. Indeed, we noticed some morphologic variation in these cultures that could alter individual cells' stretch-sensing abilities.

Because conflicting reports exist on the requirements for intracellular store release in the mechanical response of SMCs, we chose to investigate this with our stretch stimulus (Figure 4). Rat SMCs were subjected to three consecutive stretches with a 15 minute interval between stretches to minimize desensitization. In control cells, the second and third stretches reach only 80% of the peak response to the first stretch (Figure 4A, 4B). This was a consistent result seen in virtually all repeated stretch experiments with these cells and could indicate a cellular change affecting channel activity or calcium handling.

We tested the requirement for extracellular calcium in the stretch response by treating cells briefly with 2mM EGTA. If calcium enters primarily through stretch-activated ion channels on the plasma membrane, extracellular EGTA should diminish or abolish the stretch-activated intracellular calcium increase. EGTA significantly blocked the calcium response in smooth muscle to only 10% of the first stretch response, and after washout and replacement with 2mM calcium Ringer's solution the response recovered to 70% of the magnitude of control stretches (Figure 4C and 4D). This result suggests the stretch response in smooth muscle cells is mediated primarily by the opening of calcium-permeable ion channels in the plasma membrane. The small, delayed response retained in the presence of EGTA (Figure 4C) could suggest that intracellular calcium stores are contributing to the stretch response, albeit minimally and possibly due to calcium-activated calcium release (Davis et al. 1992).

To directly test the requirement for calcium store release in the stretch response of smooth muscle cells, we passively depleted stores using thapsigargin, a blocker of the SERCA calcium pump on endoplasmic reticulum. After depletion of stores (verified with subsequent application of ionomycin, data not shown) we observed that a large portion of the calcium response was retained (Figure 4E, 4F), suggesting that while stores may contribute to the magnitude of the response, they do not affect the ability of cells to respond to stretch, nor do they affect the rate of onset of the response. Taken together, these experiments demonstrate that both calcium influx and calcium stores contribute to the stretch response, but that stores are not required for this response. The calcium entering cells could be due to ion channels either directly or indirectly activated by mechanical stimuli.

Electrophysiological recordings of smooth muscle isolated from a number of different organisms have revealed the presence of channels that can be activated by suction (Wu et al. 2001) or osmotic stimulation (Langton 1993). While the identity of this channel remains unknown, it has been proposed to be a member of the TRP channel family based on its current-voltage relationship and conductance properties (Wu et al. 2001). Other studies have assigned it to the ENaC channel family based on sensitivity to the compound amiloride (Drummond et al. 2001). Pharmacological agents affecting mechanotransduction in any cell type are few, nonspecific, and often of low affinity. Conclusions can only be drawn from combinatorial studies of many agents, and the field awaits the identification of higher affinity agonists or antagonists. We chose to examine whether the compound ruthenium red (RR) affected stretch responses in smooth muscle cells. Ruthenium red is a blocker of a subset of TRP family ion channels, such as TRPV2 and TRPV4, but it can also affect store release by acting on the ryanodine receptor at high concentrations. We find that at modest concentrations of RR, the calcium response to stretch is partially blocked (Figure 5). The IC_{50} of this block is 26 μM (Figure 5B). While this is higher than the concentration known to inhibit other TRP family ion channels, it is not likely to affect ryanodine receptors at this concentration (although we did not test ryanodine-activated store release in the presence of these concentrations of RR). We can achieve partial recovery of the stretch response after washout (Figure 5D). This suggests that a RR-sensitive target is involved in the stretch response in smooth muscle cells.

One potential mechanism for stretch-activated calcium entry is by activating purinergic signaling with the release of ATP. ATP could activate either P2X (ionotropic)

or P2Y (metabotropic) receptors in an autocrine fashion on smooth muscle cells and in a paracrine fashion on visceral afferent neurons. This mechanism has been suggested to mediate bladder smooth muscle contraction response due to stretch (Cockayne et al. 2000; Vlaskovska et al. 2001). We asked whether treatment with apyrase, which hydrolyzes ATP to AMP and pyrophosphate, would reduce or eliminate the stretch response in smooth muscle cells. At concentrations that effectively inhibited ATP activation of P2X2 (data not shown), apyrase had no effect on stretch-induced calcium rise (Figure 6). This result suggests that ATP-mediated signaling does not play a significant role in initiating the stretch response in SMC.

Based on the data above, we hypothesized that a ruthenium red sensitive ion channel might be involved in transducing stretch in SMC. Two plausible channels that fit this criteria are TRPV2 and TRPV4. Both channels are members of the TRP channel superfamily involved in a myriad of sensory transduction events. TRPV2 has been proposed to play a role in sensing osmolarity and other mechanical stimuli in cardiac myocytes (Muraki et al. 2003), while TRPV4 is an osmolarity sensor in many cell types (Strotmann et al. 2000; Suzuki et al. 2003). Both are expressed in various lines of smooth muscle (Beech 2005). We first verified expression by RT-PCR in rat aorta-derived SMC of TRPV2, TRPV4, and another family member, TRPC1, that has been suggested to be a mechanosensor in certain vertebrate systems (Maroto et al. 2005). We were able to detect expression of all three TRP channels in brain RNA (positive control) and in rat SMC (Figure 7A). We tested whether TRPV2 or TRPV4 could confer stretch-induced calcium influx when heterologously expressed in HEK 293T cells (Figure 7B and 7C). Although both TRPV2 and TRPV4 were functionally expressed as verified by

treatment with 2-APB and 30% hypo-osmotic stimuli, respectively, we were unable to activate these cells with stretch stimuli. While this result suggests that these channels cannot mediate the stretch response in isolation, they could still be involved in a multi-component response. We are currently testing the responses of primary aorta-derived smooth muscle cells from TRPV2 and TRPV4 knockout mice. If these channels are involved in smooth muscle mechanotransduction, the responses from cells derived from the knockouts should reveal a deficiency in the stretch assay.

In many cell types, the styryl pyridinium dye FM 1-43 can label mechanically responsive cells in an activity-dependent manner (Gale et al. 2001; Meyers et al. 2003). FM 1-43 is a hydrophobic molecule with two positive charges. Some studies suggest that FM 1-43 labeling involves permation through a stretch-activated ion channel (Gale et al. 2001; Drew et al. 2007). Because FM 1-43 is a long-lived marker of a mechanically active cell, it could be an extremely useful tool in screening for mechanosensitive molecules. We tested if, under conditions known to activate calcium influx in SMC, we could also observe FM 1-43 cell labeling. Using three 2-second pulses of stretch, we see robust cell labeling in a punctate pattern suggesting dye accumulation on vesicle membranes (Figure 8). At this resolution we are unable to distinguish dye accumulation on the inner leaflet (suggesting endocytosis) or outer leaflet (suggesting channel permeation) of the vesicle membrane. This result does not give us additional information on the identity of the mechanosensitive ion channel, since FM 1-43 labeling has achieved by activation of TRPV1 and P2X2 (Meyers et al. 2003) and because most ion channels have not been tested in this assay. However, the ability of rat SMC to label with FM 1-43 enables the design of screens to identify proteins mediating

mechanotransduction in these cells in a higher throughput way than calcium imaging alone would allow. Furthermore, it serves as an additional verification that the smooth muscle response is indeed a plasma membrane mediated event.

Discussion

Taken together, these results suggest that calcium entry into smooth muscle cells during mechanical stimulation is mediated by a ruthenium red sensitive ion channel on the plasma membrane, with minor contributions from intracellular calcium stores. The mechanism of activation does not rely on purinergic signaling mechanisms. While our data do not identify the ion channel involved, they are consistent with the involvement of a TRP family ion channel. We have heterologously expressed a number of TRP channels without being able to produce stretch sensitivity (Figure 7 and data not shown). Testing appropriate knockout models will be important to implicate any of these channels in mechanosensation in this (or any) cell type.

Our ability to label smooth muscle cells with FM 1-43 is a technical advancement that will make screening for molecules easier because it relieves the necessity for live imaging to detect responsive cells. We have conducted an expression cloning screen based on these results. To do this, we expressed pools of cDNAs from somatosensory neurons in HEK 293T cells and stretched these cells in the presence of FM 1-43 using the 3x2sec protocol described above. This resulted in labeling in a small fraction of pools, which were then fractionated to narrow down the possible transcripts mediating this effect (see Figure 22). While we have not yet identified any candidates using this method, FM 1-43 can be used in other types of screens. For example, an RNA interference screen could be conducted in a plate-reader formatted assay designed to look for loss of FM 1-

43 labeling in stretched SMCs. The homogeneity of smooth muscle cell stretch responses simplifies the design of such a screen and allows for greater reproducibility. We have also begun to make a cDNA library from smooth muscle cells in order to screen for muscle-specific mechanosensitive molecules and have screened a few pools of this library in the aforementioned expression cloning approach.

On a larger level, we have demonstrated the use of an easy, reproducible live imaging system for the study of mechanosensation in virtually any adherent cell type. This system is a technical advancement over previous methods because of the ease of stimulating and imaging large numbers of cells uniformly in real time. It may represent a novel way of mechanically stimulating cells. While it is difficult to compare stretch stimulation with other mechanical stimulation methods such as suction of a patch of membrane or poking of a cell with a polished pipette, we believe that stretch and other mechanical stimulation methods activate similar response mechanisms. Two likely differences are that stretch of cell bodies likely stimulates a larger portion of the membrane than does suction or poking with a pipette, and that stretch responses rely strongly on adhesion of cells through molecules like integrins or focal adhesion complexes. Stretch stimulation of cultures over time induces changes in cellular form that correlate with changes in blood vessels in vivo (Ross 1993), suggesting that in vitro stretch is a good approximation for the mechanical forces acting on these cells in their normal physiological context. However, the initial events leading to these cellular changes have been understudied to date, and the initiation of mechanical signaling still represents a “black box” in our understanding of vascular biology. Real-time calcium

imaging of stretched cultures will allow insights into the triggers that govern the myogenic response and the alterations that lead to vascular resistance and atherosclerosis.

Figure Legends

Figure 2. Smooth muscle cells respond to stretch in culture. (A, left panel) Smooth muscle cells before stretch, showing low levels of internal calcium. Colored bar shows pseudocolor scale, with lowest calcium at bottom. (A, right panel) The same cells 2 sec after stretch, showing elevated calcium levels. Note that cells have shifted slightly due to the stretch. (B) Average trace of all cells (n=83) during a repeated 12% stretch (blue bars).

Figure 3. Smooth Muscle Cell Stretch Responses are Dose Dependent. A and C, Rat aortic smooth muscle cells at passages 18-24; B and D, mouse aortic smooth muscle cells 14 days after dissociation. A and B, Peak responses to stretches from 2.5% to 15%. Peaks were normalized to the pre-stretch baseline. Half-maximal responses (+/- SD) were obtained at a stretch of 6.6 +/- 2.1% for rat and 7.4 +/- 0.96% for mouse SMC. Each point represents the average of 100-300 cells. C and D, Percent of smooth muscle cells responsive to stretches from 2.5% to 15%. 50% of cells respond by 4.95 +/- 0.24% stretch for rat and 7.8 +/- 0.57% stretch for mouse.

Figure 4. Stretch Responses in Smooth Muscle Cells Require Extracellular Calcium and Intracellular Calcium Stores. A, Average response of rat SMC (n=73) to three consecutive stretches (vertical bars). B, Normalized responses from (A). C, Average response of rat SMC to three stretches, 1st and 3rd in 2mM Ca^{2+}, and 2nd in 2mM EGTA (orange bar). EGTA treatment was limited to 2 minutes to minimize cell detachment.

Red bar, 10μM ionomycin in 10mM Ca^{2+}. D, Normalized responses from (C). E, Stretch (vertical bars) before and during treatment with 2μM thapsigargin. Green bar, thapsigargin in 0.9μM free calcium (as calculated by MaxChelator); striped bar, thapsigargin in 2mM Ca^{2+}. Red bar, 5μM ionomycin in 10mM Ca^{2+}. In a parallel experiment, store emptying after this amount of thapsigargin treatment was confirmed by ionomycin addition (data not shown). F, Normalized responses from (E). Each stretch was normalized to its pre-stretch baseline for 30 sec before stretch, and the first stretch peak response was set to 1.

Figure 5. Ruthenium Red partially blocks the stretch-induced calcium increase in smooth muscle cells. A, Average trace of a single experiment (n=32 cells) in which the middle of three stretches (black bars) is done in 20μM Ruthenium Red (RR, red bar). B, Percent block with varying concentrations of RR. Values were normalized to the peak of the first stretch in each experiment, and all experiments were done as in (A). Error bars are SEM. C and D, Histograms of the peak responses of individual cells in pooled experiments done as in A (n=136 cells). Red in both graphs shows cell responses during 20μM RR treatment, while blue in (C) shows the first stretch and in (D) the last stretch.

Figure 6. Smooth muscle cells do not require ATP release for stretch activation. A, Average traces of cells during three stretches with no treatment (black trace) or with 0.5U/ml apyrase treatment (red bar) during the second stretch (red trace). Orange bar, ionomycin treatment. B, Quantitation of responses shown in A, normalized to the

baseline fluorescence. Maximum is taken as the control response to the first stretch and is set at 1. Error bars indicate SEM.

Figure 7. TRPV2 and TRPV4 are not stretch sensitive channels in heterologous systems. A, RT-PCR with primers specific for TRPC1, V2, and V4. Brain polyA+ mRNA was used as a positive control for primers. B, Heterologous expression of TRPV2 in HEK293T cells. 2-APB treatment (500μM, yellow bar) shows functional expression of TRPV2. C, Heterologous expression of TRPV4 in HEK293T cells. TRPV4 is functionally expressed as demonstrated by osmotic activation.

Figure 8. Smooth Muscle Cells Take Up FM 1-43 Dye In a Stretch Dependent Manner. A and B, Smooth muscle cells incubated in 10μM FM 1-43 for 90s. A, Stretched 3 x 5sec in the presence of FM 1-43. B, No stretch.

Figure 2.

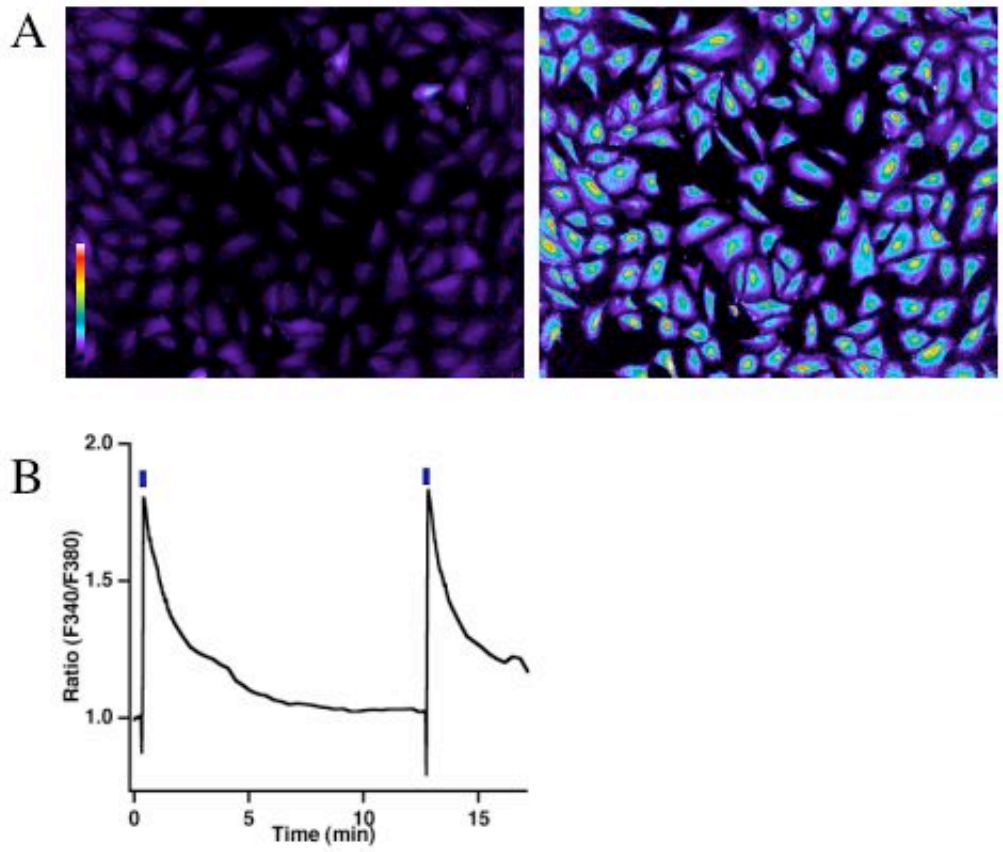

Figure 3.

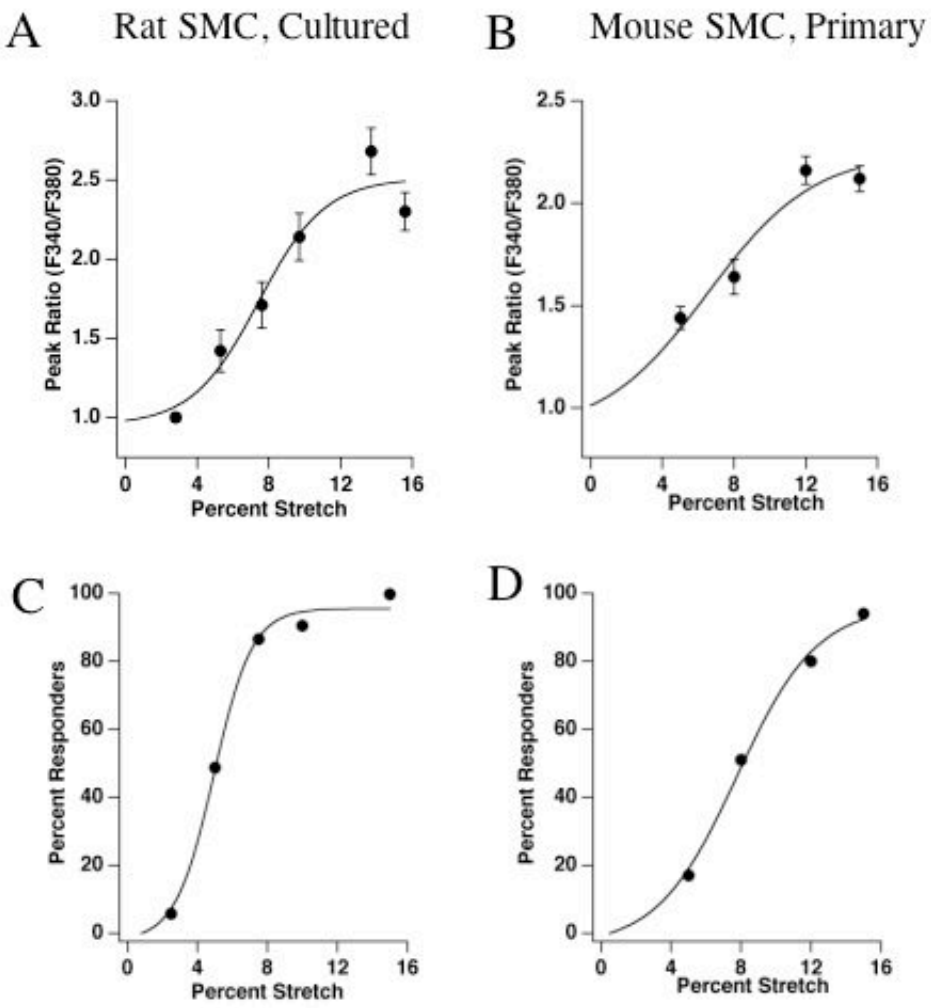
A
Rat SMC, Cultured
B
Mouse SMC, Primary
Peak Ratio (F340/F380)
Percent Stretch
C
D
Percent Responders
Percent Stretch

Figure 4.

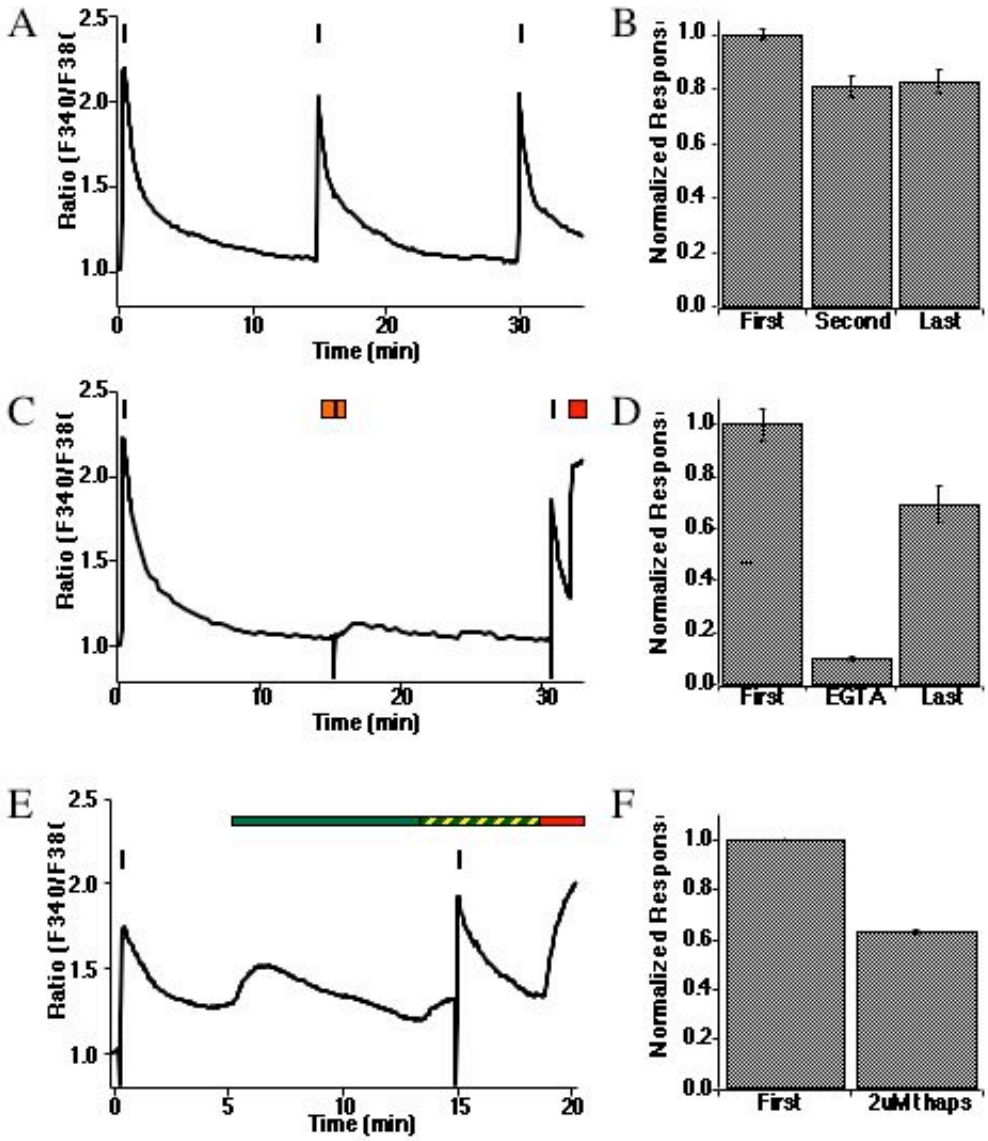
A
Ratio (F340/F38(
2.5
2.0
1.5
1.0
0
10
20
30
Time (min)
B
Normalized Respons
1.0
0.8
0.6
0.4
0.2
0.0
First
Second
Last
C
Ratio (F340/F38(
2.5
2.0
1.5
1.0
0
10
20
30
Time (min)
D
Normalized Respons
1.0
0.8
0.6
0.4
0.2
0.0
First
EGTA
Last
E
Ratio (F340/F38(
2.5
2.0
1.5
1.0
0
5
10
15
20
Time (min)
F
Normalized Respons
1.0
0.8
0.6
0.4
0.2
0.0
First
2uM thaps

Figure 5.

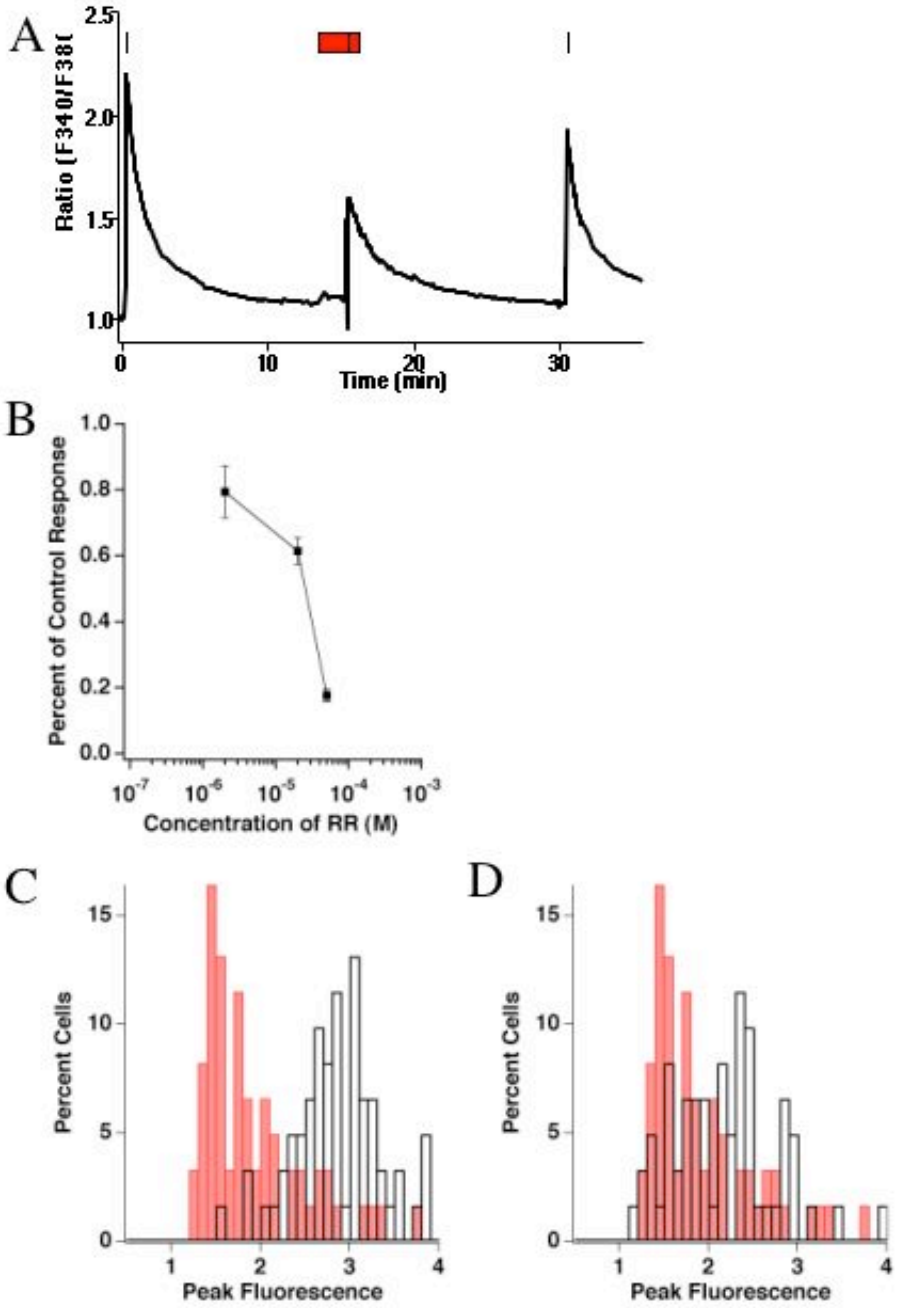
A
Ratio (F340/F38(
2.5
2.0
1.5
1.0
0
10
20
30
Time (min)
B
Percent of Control Response
1.0
0.8
0.6
0.4
0.2
0.0
10-7
10-6
10-5
10-4
10-3
Concentration of RR (M)
C
Percent Cells
15
10
5
0
1
2
3
4
Peak Fluorescence
D
Percent Cells
15
10
5
0
1
2
3
4
Peak Fluorescence

Figure 6.

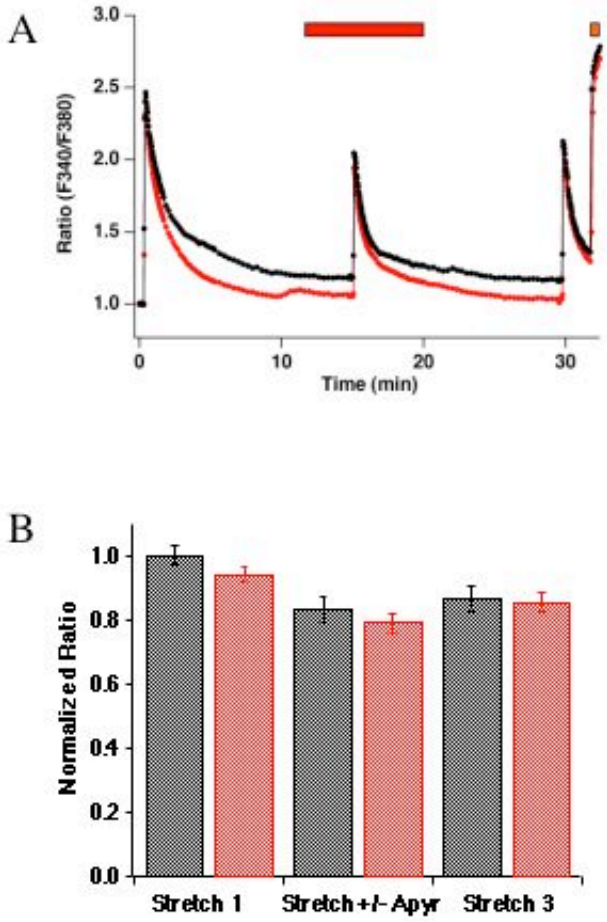
A
3.0
2.5
2.0
1.5
1.0
Ratio (F340/F380)
0
10
20
30
Time (min)
B
1.0
0.8
0.6
0.4
0.2
0.0
Normalized Ratio
Stretch 1
Stretch +/- Apyr
Stretch 3

Figure 7.

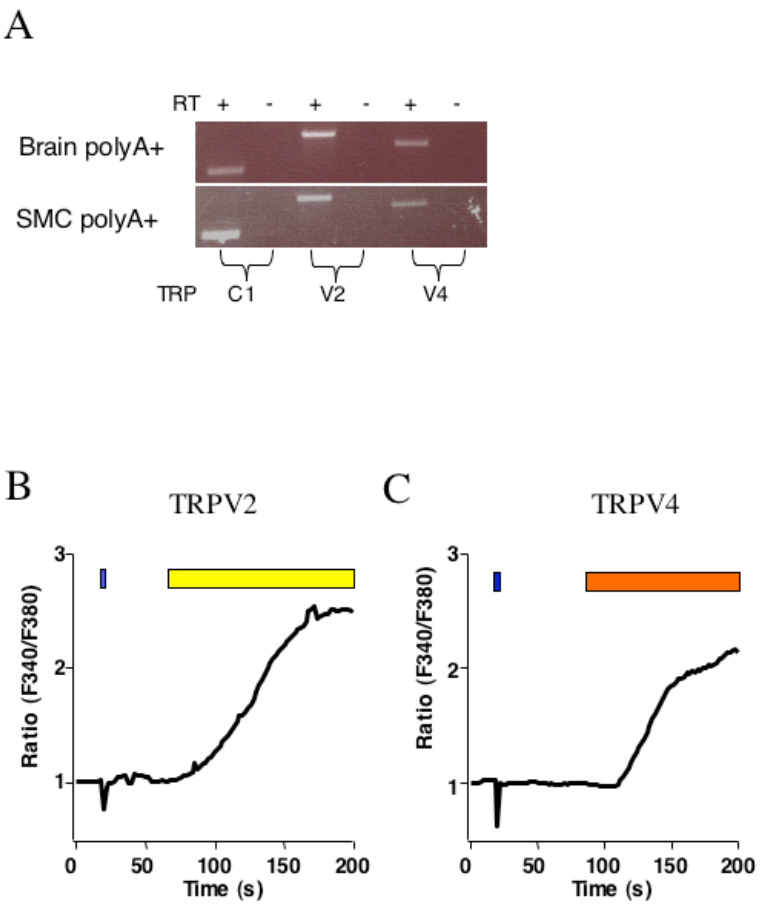
A
RT + - + - + -
Brain polyA+
SMC polyA+
TRP C1 V2 V4
B
TRPV2
Ratio (F340/F380)
Time (s)
C
TRPV4
Ratio (F340/F380)
Time (s)

Figure 8.

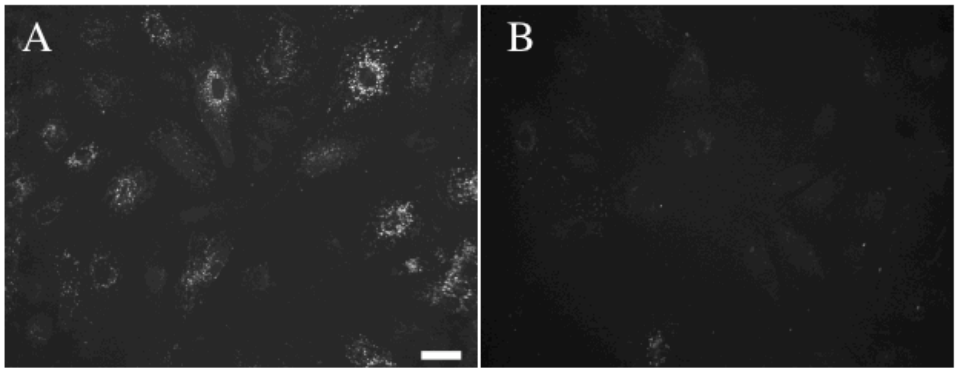

CHAPTER THREE

STRETCH EVOKED CALCIUM TRANSIENTS DEFINE A NOVEL POPULATION OF MECHANOSENSORY NEURONS

Introduction

Somatosensory neurons are uniquely positioned to detect mechanical stimuli in the form of touch and proprioception. These neurons, with cell bodies in the dorsal root ganglion (DRG) and trigeminal ganglion (TG), are pseudo-bipolar in nature, with one long dendrite projecting to near the skin's surface and one axon projecting to the spinal cord. The dendrite takes on varying morphologies once it arrives in the epidermis or dermis, and these morophologies affect the types of mechanical stimuli it transduces. For example, neurons innervating Pacinian corpuscles are positioned deep in the skin and respond most readily to fast vibrations and rough textures, while neuronal endings in Merkel cell-neurite complexes reside at the dermis-epidermis interface and respond to more gentle stimuli. These morphological features are complemented by a wide range of neuronal properties that can modify responses to similar stimuli. Pacinian corpuscle dendrites adapt quickly to the onset of a mechcanical force (rapidly adapting (RA) responses), while neurons in Merkel cell complexes continue to respond to a sustained stimulus (slowly adapting (SA) responses). This diversity of neuronal types and ending morphologies affords us the spatial and dynamic range necessary to respond to a wide variety of mechanical stimuli.

Both molecular markers and intrinsic neuronal properties like conduction velocity can be used to classify somatosensory neurons into functional categories. In studies of mechanosensation, neurons are often categorized by their adaptation properties (RA, SA, and intermediate) and by the mechanical threshold necessary to evoke action potentials, qualities which emerge from electrophysiological studies of mechanically gated currents and/or the resulting action potential firing (Lumpkin et al. 2005). While these measures

reveal significant information about channel properties and coding of a mechanical stimulus, they are tedious cell-by-cell analyses that often are insufficient to accurately report population fractions.

Some of the best molecular markers can be used to functionally delineate sensory neuron categories in calcium imaging assays. For example, the capsaicin receptor TRPV1 is found in about 60% of dissociated DRG and TG neurons by calcium imaging, a number that corresponds well with immunohistochemical staining in intact ganglia (Caterina et al. 1997). Capsaicin responsiveness defines a group of unmyelinated, polymodal nociceptors (C-fibers). This category can be further divided into those neurons containing neuropeptides (peptidergic) and those that do not; antibodies to peptide markers like Substance P can identify these subgroups.

Studies characterizing mechanically gated currents in sensory neurons report varying percentages of neurons that respond to force; these numbers likely reflect differences in the stimuli used to obtain them. Using positive pressure in the whole-cell recording configuration, about 30% of neurons respond to increases in pressure, although high pressures were limited by the fragility of cells (Cho et al. 2002). The same study reports that 47% of neurons contain either low or high-threshold mechanosensitive currents in cell-attached patch configuration. In contrast, poking neurons with a polished glass pipette results in 92-95% of cultured sensory neurons responding (Drew et al. 2002; Hu et al. 2006; Wetzel et al. 2007). This percentage is also reported to be sensitive in the skin-nerve preparation (Wetzel et al. 2007). In studies using low osmolarity as a mechanical stimulus, 78% are reported to respond by calcium imaging (Viana et al. 2001). These discrepancies are probably reflective of different magnitudes of mechanical

stimuli in each study, a parameter which has yet to be normalized across varying types of force (osmotic, suction, deformation, and stretch).

Molecular markers for mechanosensitive somatosensory neurons have been lacking, in part due to the discrepancies in reports on which cells are sensitive to mechanical stimuli and in part due to the low throughput nature of most of these stimuli. Poke stimulation of mechanosensitive currents in rat DRG neurons suggests that capsaicin positive RA neurons have higher thresholds and lower peak currents than do capsaicin negative RA neurons, and that within capsaicin positive neurons, those that label with the isolectin IB4 (nonpeptidergic nociceptors) are much less sensitive to this mechanical stimulus (Drew et al. 2002). Osmotically sensitive TG neurons, in contrast, did not seem to reside preferentially in capsaicin positive or negative populations (Viana et al. 2001). Both of these studies investigated 100 neurons or less in coming to their conclusions and therefore the response percentages reported are susceptible to significant sampling error. The NT3 growth factor receptor TrkC marks Aδ and Aβ mechanoreceptors (Funfschilling et al. 2004), but the mechanosensitive properties of this subset have not been directly tested. In recent years, many additional markers have been identified and could shed light on the populations responding to touch (McKemy et al. 2002; Jordt et al. 2004).

In developing the stretch assay described in the previous chapter, we realized that higher throughput methods were necessary to fully characterize mechanosensory neurons and other mechanosensitive cell types. Furthermore, in order to screen for molecules involved in these processes, a high-throughput functional assay is necessary. While chemical agents purported to stretch the cell membrane (including low osmolarity and

amphipathic/crenator molecules) could be used, these do not mimic the responses or kinetics that are observed with physical methods of stretch (Viana et al. 2001). Therefore, such agonists may not be appropriate for identifying molecules responsible for the fast currents evoked by physical methods. Indeed, expression cloning screens using low osmolarity stimuli have not identified mechanosensitive channels (Caprini et al. 2003).

We sought to use stretch as a functional assay for populations of mechanosensitive channels. In particular, we wanted to assess the validity of this stimulus in detecting populations of mechanosensitive cells. Furthermore, we hoped to identify characteristics of stretch-activated signaling in sensory neurons that could inform the identification of molecules involved in stretch responses.

Results

A transient stretch of two seconds is sufficient to activate a transient rise in intracellular calcium in cultured neonatal trigeminal neurons (Figure 9A and 9B). Not all neurons are competent to respond to stretch stimulation, even at high magnitudes of stretch. These neurons are still able to depolarize in response to high potassium solution to a similar degree as stretch responders, suggesting that they are simply not stretch sensitive. Interestingly, we find that individual cells begin responding at different magnitudes of stretch (Figure 9A,B,C). This result implies that different subsets of sensory neurons may exhibit unique mechanical thresholds in culture. It also illustrates that cells are competent to respond to multiple stretch stimuli in relatively short succession.

Low amounts of stretch (10% increase in cell diameter) activate about 5% of sensory neurons, whereas high amounts of stretch (14% increase in cell diameter)

activate about 20% of trigeminal neurons (Figure 9C). Additional stretch does not continue to recruit new responders, suggesting that we have identified the entire population of stretch-sensitive neurons. This percentage is slightly lower than that reported in studies using whole-cell positive pressure to stimulate neurons (Cho et al. 2002). We see that virtually all cells responding to 10% stretch also respond to 14% stretch (for example, Figure 9B), suggesting that once the threshold for activation is exceeded, cells will respond to all stretches.

Analysis of peak responses to varying stretch stimuli shows very little difference in magnitude between low-threshold and high-threshold responders as a population (Figure 9E). Similarly, we observed no change in average size of cells responding to lower and high stretches (Figure 9D). However, these analysis fail to consider the response threshold. Indeed, individual low-threshold responders demonstrate increases in response magnitude with increasing percentage stretch (Figure 9B, Figure 10). If responders are classified based on their initial response threshold, the magnitude of their responses at high stretch are significantly different, with low-threshold responders showing much larger responses to higher stimuli than high-threshold responders (Figure 10C). This response is similar to graded responses in other sensory systems that precede action potential generation. The graded nature of these responses in addition to their modest size suggests that these calcium transients are reflective of transduction and may not require large amounts of amplification by voltage-gated channels. Pharmacological block of different populations of voltage gated calcium channels should further clarify the source of calcium in these stretch-induced transients.

We sought to characterize the population of neurons that responds to stretch using functional markers for distinct subpopulations of these neurons. Capsaicin activates 60% of sensory neurons in culture, and these cells are generally considered nociceptors. We hypothesized that higher stretches would activate mechano-nociceptive neurons that express the capsaicin receptor TRPV1. We find that capsaicin sensitivity partially overlaps with stretch sensitivity, with the degree of overlap dependent on stretch magnitude (Figure 11). An increase in capsaicin-sensitive stretch responders with increasing stretch magnitude indicates that nociceptive neurons are being recruited into the stretch-sensitive population as higher stretches are applied (Figure 11B). Thus the amounts of stretch used are sufficiently high to activate pain sensing neurons, and, predictably, these nociceptive neurons generally have higher mechanical thresholds. Remarkably, we find no overlap with menthol-sensitive TRPM8-positive neurons nor with mustard oil-sensitive TRPA1-positive neurons (Figure 11C). TRPA1 has been previously proposed to be a mechanosensitive channel (Corey et al. 2004), but TRPA1 knockout animals show normal responses to behavioral measures of touch sensation (Bautista et al. 2006). The lack of co-localization of stretch and mustard oil responsiveness, coupled with normal stretch responses in neurons from TRPA1 knockout animals (data not shown), demonstrates that TRPA1 is not involved in the stretch response.

Because a portion of stretch sensitive neurons do not seem to be nociceptors (based on TRPV1 expression and lower mechanical thresholds), we sought markers of this population. A recently identified compound from the Szechuan peppercorn, hydroxy-α-sanshool (hereafter called sanshool), induces calcium influx in approximately

50% of cultured sensory neurons (Diana Bautista, unpublished data). This molecule has been proposed to be a chemical mimic of physical mechanical stimuli due to its ability to evoke tingling sensations (Bryant et al. 1999). We observed that stretch-sensitive neurons are highly sensitive to sanshool (Figure 12A). In neurons that respond to 10% stretch, 95% are also responsive to sanshool (Figure 12B). Sanshool activates about 50% of sensory neurons, and it is important to note that most of them remain unresponsive to stretch, even at higher stimulus magnitudes. Thus stretch and sanshool likely operate through distinct mechanisms. Stretch activates cells in capsaicin-positive and capsaicin-negative subgroups of sanshool responders. With larger stretches, the total number of capsaicin positive neurons increases (as seen in Figure 11) and the percentage of sanshool positive neurons decreases, reflecting the recruitment of nociceptors that are not responsive to sanshool (Figure 12C). These results show that there are two main populations of stretch-sensitive sensory neurons: sanshool positive low threshold stretch receptors, and capsaicin positive high threshold stretch receptors. While these populations overlap (i.e. the sanshool-positive cap-positive neurons), it is clear that sanshool and capsaicin are the primary hallmarks of these subsets of stretch responsive neurons.

In addition to these chemical stimuli, we wanted to know if methods used to mimic mechanical forces would activate similar subsets of neurons as stretch. In vivo, cells are normally bathed in extracellular solutions with osmotic strengths of about 300 mOsm. Reducing the osmotic strength surrounding cells can activate currents and calcium influx in many cell types, including sensory neurons (Viana et al. 2001; Pasantes-Morales et al. 2006). The mechanism by which these changes occur is

relatively unclear, but in some cell types TRP channels such as TRPV2 (Muraki et al. 2003) and TRPV4 (Strotmann et al. 2000; Mizuno et al. 2003) are suggested to be primary osmosensory channels. We find that all stretch-sensitive TG neurons are also sensitive to low osmolarity (Figure 13A and 13B). Similar to sanshool, the stretch-sensitive population is a subset of a larger osmosensitive population of neurons, and thus it is unlikely that osmolarity and stretch operate through the same mechanisms. This finding is interesting in that it correlates two types of mechanical stimulation. However, the membrane stretch that occurs during osmotic swelling could be physically distinct from the stretch of cell membrane imposed on cells in our assay. Without precise measurements as to how cell shape changes during osmotic stimuli or stretch, we cannot compare the magnitudes of these different stimuli in terms of membrane force. We have modeled cell shape and volume of neurons using confocal microscopy before and during stretch and have not observed significant differences in these parameters (data not shown).

Because sanshool activates a population of neurons that expresses the neurotrophin-3 receptor Trk-C, we hypothesized that a subset of the stretch sensitive population would contain this receptor. Trk-C is expressed in a subset of neurons containing low-threshold mechanosensitive neurons and proprioceptive neurons, and its signaling is required for the proper development of this population (Klein et al. 1994). To test our hypothesis, we stretched neurons from mice that express GFP in Trk-C expressing cells (Funfschilling et al. 2004). We observed that, while all stretch sensitive cells are not Trk-C+, there is an enrichment of GFP expression in stretch responders compared to the total population (Figure 13C and 13D). The lack of total colocalization

is expected because nociceptive neurons, such as those expressing TRPV1 and responding to capsaicin, are also responsive to stretch and are dependent on TrkA, not Trk-C, signaling. Supporting this idea, enrichment in TrkC+ neurons peaks at 10% stretch and does not increase further with 14% stretch (Figure 13D).

Increased intracellular calcium in sensory neurons following stretch could result from entry through ion channels in the plasma membrane or from release of calcium stores in the endoplasmic reticulum, or a combination of these two mechanisms. To identify the source of calcium responsible for stretch-induced calcium transients, we removed all extracellular calcium and replaced it with EGTA, a calcium chelator. We find that stretching these neurons results in no responses in any sensory neurons (Figure 14A and 14B). Replacement of the EGTA solution with solution containing calcium rescued the responsiveness of these neurons. Importantly, we minimized the duration of EGTA treatment to reduce the possibility that EGTA would disrupt cell adhesion and thus reduce or eliminate stretch responses. Because we are able to see complete block and recovery from block within the span of one minute, we believe that the elimination of the stretch response reflects a lack of calcium rather than a lack of adhesion. Thus, we believe that stretch causes influx of calcium through a calcium-permeable ion channel. This result is consistent with reports measuring nonselective cation currents evoked by mechanical stimuli (McCarter et al. 1999; Takahashi et al. 2000; Cho et al. 2002).

Mechanical responses in many types of cells can be blocked by the trivalent ion gadolinium (Gd^{3+}). This ion is an extremely promiscuous blocker of many types of channels, and it is not useful in distinguishing mechanosensitive channels from other types of channels, despite wide citation as a mechanosensitive channel blocker.

However, block by this ion would further support the hypothesis that our stretch responses are due to permeation through an ion channel rather than through transient leakiness or injury to cells. We find that application of Gd^{3+} causes complete block of stretch responses in sensory neurons (Figure 14C and 14D). This ion also blocks depolarization induced by high potassium solutions, indicative of its capacity to block many types of channels. Taken together with our results in EGTA, we conclude that we are witnessing the activity of a calcium-permeable plasma membrane ion channel.

Mechanosensitive currents in sensory neurons due to poking are blocked by low concentrations of Ruthenium Red (Drew et al. 2002), a molecule that blocks a number of calcium permeable channels including some types of TRP channels, voltage gated channels, ryanodine receptors and the mitochondrial calcium uniporter (Bernardi et al. 1984; Cibulsky et al. 1999; Xu et al. 1999; Ramsey et al. 2006). We hypothesized that if poking and stretch activate similar mechanisms, ruthenium red would block stretch-induced calcium influx. We found that concentrations over three times those reported to block poke responses did not change the percentage or magnitude of stretch responses (Figure 15). This could be due to a difference in the quality of the stimulus, since poking activates over 90% of sensory neurons in culture (Drew et al. 2002), while we observe 20% responding to stretch (Figure 9C). Our results also suggest that ruthenium red sensitive ion channels such as TRPA1 and TRPV1 are not involved in the stretch response.

We sought to extend our analysis of sensory mechanisms to neurons of the dorsal root ganglia (DRG). DRG neurons innervate the majority of the skin on the body, whereas trigeminal neurons innervate only the facial area. We found that, after three

days in culture, DRG cell bodies show stretch activation that is virtually identical to that found in trigeminal neurons (Figure 16A and 16B). In addition, the stretch-response curve for DRGs and trigeminal neurons are quite similar at low stretches, with DRGs showing higher percentages of stretch-sensitive cells at high stretches (Figure 16C). We conclude that the mechanisms mediating stretch sensitivity in these two types of somatosensory neurons are likely identical. Definitive differences between these two cell types have not been shown for temperature or chemical stimuli like capsaicin, and thus our stretch results fit well with the interpretation that these cell types are functionally homologous.

Behavioral models for altered mechanotransduction properties during injury are well established for areas innervated by DRG dendrites. Inflammation induced by injection of substances such as Complete Freund's Adjuvant (CFA), injury to the sciatic nerve, or infection with Varicella zoster virus can lead to transcriptional and functional changes in DRG neurons and in the spinal cord that affect touch behaviors (Waxman et al. 1999; Breese et al. 2005; Garry et al. 2005). We asked whether inducing inflammation in vivo through CFA injection could affect stretch activation of DRG neurons. Mice injected with CFA showed clear behavioral phenotypes to the injection such as paw licking and enhanced sensitivity to Von Frey filaments (data not shown). However, neither the percentage nor the peak stretch responses of DRG neurons were significantly altered under these conditions of inflammation (Figure 17). It is possible that the necessity to culture these neurons for three days before stretching allows neurons to recover from the inflammatory assault in vivo. Applying a stimulus such as poking or

suction immediately after dissociation could reveal any short term changes in mechanical sensitivity occurring in DRG neurons.

Discussion

Using a mechanical stimulus that can simultaneously activate hundreds of cells at once, we have been able to thoroughly characterize the subset of somatosensory neurons that is capable of responding to stretch stimulation. Interestingly, this population does not encompass all neurons but is restricted to a subset that is definable by molecular markers, a result that contrasts with studies using other types of stimuli that activate many more neurons. The answer to whether all somatosensory neurons are mechanosensitive clearly depends on the assay used to detect responses. Our stretch system relies entirely on the detection of an intracellular calcium rise by the reporter dye Fura-2. Many possibilities exist for the discrepancy in percent of neurons responding to stretch versus other stimuli. Two major technical factors limit the resolution of our assay: ratiometric imaging and focal changes during stretch. Using a ratiometric dye limits the time resolution of our imaging to about 1 second per frame. This acquisition speed can cause bleaching of the dye (data not shown) and we therefore limited our experiments to two or three seconds between frames. Secondly, a change in the focal plane of the cells occurs naturally during stretch of the silicone membrane. While a post underneath the membrane minimizes movement in the Z direction, the membrane nevertheless becomes thinner and drops below the plane of focus. Due to these factors, it is likely that the peak of the stretch response is missed. In addition, during our analysis we do not consider the first frame after return to focus because of a movement artifact that often occurs in this plane, and in disregarding this data point we increase the chance

of underestimating the peak or percentage of neurons responding. In summary, we may lose fast responses that recover quickly in the period during or immediately following stretch due to a combination of technical and analytical issues.

The K_d of Fura-2 in cells is approximately 1μM and quantification is most accurate within a few hundred nanomolar of this value. This range is adequate for the cell types that we have tested and reports a 5 to 8-fold change in ratio when calcium concentrations are varied from 0 (2mM EGTA) to 10mM. However, given the tight affinity of this dye for calcium, the dissociation rate could limit detection of very rapid changes in calcium concentration. In addition, currents from some mechanosensitive channels are reported to be more permeable to other cations than to calcium (Cho et al. 2002). Thus, many mechanosensitive channels must open in order to visualize a calcium signal in sensory neurons. This resolution is much less than that achieved in cell-attached patches, where single channel events can be observed, and may be reflected in the number of stretch responders.

We find that sensory neurons activated by stretch can be classified based on their activation threshold (Figure 10) and sensitivity to chemical agonists (Figure 11, 12, and 13). An intriguing finding is that stretch responders are subsets of responders to two other pseudo-mechanical stimuli: the "tingling" agent hydroxy-alpha-sanshool and hypotonic solutions. This raises the possibility that stretch-activated ion channels could be related to those responsible for the sanshool and hypotonic responses. However, sanshool does not activate all stretch responders at larger stimulus magnitudes, whereas hypotonic solutions activate all low and high threshold stretch responders. At concentrations of 100μM sanshool activates about 50% of DRG neurons in culture, but higher

concentrations are reported to activate virtually all DRG neurons (Koo et al. 2007). With respect to osmolarity, we suggest that mechanisms other than membrane stretch could be involved in some or all sensory neurons to cause intracellular calcium increases in response to hypotonic solutions. Cell swelling will change the effective concentrations of signaling components and could affect many types of chemical reactions within the cytoplasm. We propose that stretch represents a more representative stimulus for a sensory neuron than does low osmolarity, with stretch being a purely physical stimulus and one to which sensory nerve endings are exposed during the sense of touch.

While we have been unable to observe block with specific agonists, we see complete block of stretch responses when extracellular calcium is unavailable or when nonspecific calcium channel antagonists such as gadolinium ions are present (Figure 14). These observations argue strongly that calcium influx through a calcium-permeable ion channel, rather than store release or transient membrane injury, is responsible for the responses we see by calcium imaging. The ability of cells to respond to consecutive stretches also argues against attributing these responses to injury. It is likely that we are witnessing the mechanotransduction receptor potential in these cells because we see small, transient, and graded responses. However, we have yet to formally prove this by blocking voltage-gated channels or depleting intracellular stores and examining the remaining stretch response.

A recent report suggests that neurites of sensory neurons in culture are more mechanosensitive than the cell bodies (Hu et al. 2006). This finding is intriguing and may be a useful model for the in vitro study of mechanosensitive currents in structures similar to sensory nerve endings. We have begun to assess whether calcium signals are

detectable in neuronal processes in culture and are able to observe capsaicin evoked signals at the junctions of subsets of these neurites (data not shown). However, not all neurons in culture appear to regrow neurites, and those with undetectable neurites are still able to respond to stretch. Thus while there could be an enrichment of mechanosensitive channels in these processes, it is likely that stretch stimulates channels in the cell bodies as well.

The extension of the use of stretch to the study of sensory neuron mechanotransduction is a long overdue application of a stimulus that has been well documented to activate mechanosensitive channels in other cell types. It has allowed a thorough characterization of the types of sensory neurons competent to respond to mechanical stimulation, an analysis which has been lacking due to the low throughput of other physical stimulus methods. Stretch is capable of activating cells with a range of stretch thresholds, including large diameter low-threshold touch receptors, proprioceptors, and nociceptors. Furthermore, the development of this stimulus allows for the high-throughput analyses of library pools made from sensory neurons, and in the future this may enable the identification of sensory neuron mechanotransduction channels.

Figure Legends

Figure 9. Stretch activates a subpopulation of trigeminal sensory neurons. A, timelapse ratio images of Fura-2 loaded trigeminal sensory neurons at the following points: (1) before stretch, (2) 3 s after a 14% stretch (2 s), (3) after 1min recovery, (4) 3 s after a second 14% stretch (2 s), and (5) during 75mM K+ Ringer perfusion to activate all neurons. Responders are noted with arrows. B, trace of a single neuron shown in (A) (red arrow) showing time course of responses to two 14% stretches (black bars). Yellow bar, high potassium Ringer. Dotted lines show points where images in (A) were taken. C, Percentage of all neurons that respond to varying stretches. Data were compiled from the first stretch of many experiments. Error bars are SEM. D, Average diameter of stretch responders at different amounts of stretch. Error bars are standard deviation. E, Normalized peak responses to varying amounts of stretch. Error bars are SEM.

Figure 10. Stretch threshold correlates with peak responses to high stretch. A, Pseudocolor images of neurons stretched at four different magnitudes. (1) start, (2) 8% stretch, (3) 10% stretch, (4) 11.5% stretch, (5) 13% stretch (6) High K+. B, Two representative neurons with different stretch thresholds. Red trace, top responsive neuron in (A) with a threshold of less than 8% stretch. Black trace, bottom responsive neuron in (A) with a threshold of 11.5% stretch. Black bars show stretch duration (2 s). B, Quantification of the peak stretch responses at 13% stretch in neurons with either an 8% (n=11) or 13% (n=30) stretch threshold. Data is from experiments done as in A. Error bars are SEM.

Figure 11. Stretch responders include TRPV1-expressing nociceptors. A, Neuron that is stimulated with 10% stretch (light blue bar), 14% stretch (dark blue bar), capsaicin (red bar) and high potassium Ringer (yellow bar). B, Quantification of the percent of stretch responders that also respond to capsaicin at 10% stretch and 14% stretch. Error bars represent SEM. C, Quantification of the percent of stretch responders that also respond to menthol or mustard oil at 14% stretch. No overlap of these agonists with stretch was observed.

Figure 12. Hydroxy-alpha-sanshool activates low threshold stretch sensitive neurons. A, Representative neuron showing a stretch response at 14% stretch (blue bar) followed by treatment with sanshool (purple), cap (red) and high potassium ringer (yellow). B, Percentages of stretch sensitive cells that are also activated by sanshool, capsaicin, or both at 10% stretch. Experiments were done as in A. C, Percentages of stretch sensitive cells that are also activated by sanshool, capsaicin, or both at 14% stretch.

Figure 13. Stretch responders are sensitive to hypotonic stimuli and contain Trk-C positive neurons. A, Representative neuron showing a response to 14% stretch and to 215mOsm Ringer. B, Quantification of many experiments done as in A. Osmolarity activates a larger percentage of neurons than does stretch. All stretch responders are also osmosensitive. C, neurons dissected from mice expressing EGFP under the control of Trk-C-Cre. Middle image, 14% stretch. Right image, GFP. D, Totals of all Trk-C-EGFP neurons analyzed, showing the percent of GFP positive neurons activated by 10% or 14%

stretch. Neurons were counted as GFP positive if their fluorescence was at least 1.5x the average fluorescence of a clearly negative neuron in the same field.

Figure 14. Neuronal stretch responses can be eliminated by EGTA and gadolinium treatment. A, individual neuron stimulated with 14% stretch (black bars) while in 2mM EGTA (blue bar) or after washout with 2mM calcium. B, Quantification of all experiments done as in (A), n=39. Error is SEM. C, individual neuron stimulated with 14% stretch (black bars) in the absence or presence (orange bar) of 10μM $GdCl_3$. Yellow bar, high potassium ringer. D, Quantification of peaks before and during $GdCl_3$ application as in (C), n=7. Error is SEM.

Figure 15. Ruthenium Red treatment does not affect the neuronal stretch response. A, two cells responding to 14% stretch in the presence of 10μM ruthenium red (red bar) and after washout. Yellow bar, high potassium ringer. B, Quantification of average peaks of all responders in the experiment shown in A and in a control experiment without ruthenium red done on the same day. Only first stretches were used in this analysis. Error bars are SEM.

Figure 16. Neurons from the dorsal root ganglia have similar responses to those from the trigeminal ganglia. A, series of still images from an experiment before (left panel) and immediately after 9% and 13% stretch. White arrow, a neuron that responds at 9% stretch. Pink arrows, neurons that have little to no response at 9% but a noticeable response at 13% stretch. Right panel, depolarization with 75mM K+ Ringer. In order to

show small stretch responses, the pseudocolor range of all images was adjusted, resulting in the appearance of saturation during depolarization. B, representative trace of a DRG neuron responding to both 10% and 14% stretch stimuli. C, stretch-response curve of DRG neurons. Error bars represent SEM.

Figure 17. CFA injection in vivo does not sensitize DRG neurons to stretch. Mice were injected with 1:1 CFA in PBS or PBS alone (sham), and ganglia from the affected lumbar regions (L4-L6) were dissociated. A, percentage of neurons responding at various stimulus levels in CFA and sham-injected mice. Various stimulus protocols were used in data acquisition, with the first stretch at 5% or 10% and the second stretch at 15% or 18%. Error bars are SEM of individual trials. B, normalized peak responses of responding DRG neurons to various stretches. Data gathered as in A. Error bars are SEM of the peaks of all responding neurons.

Figure 9.

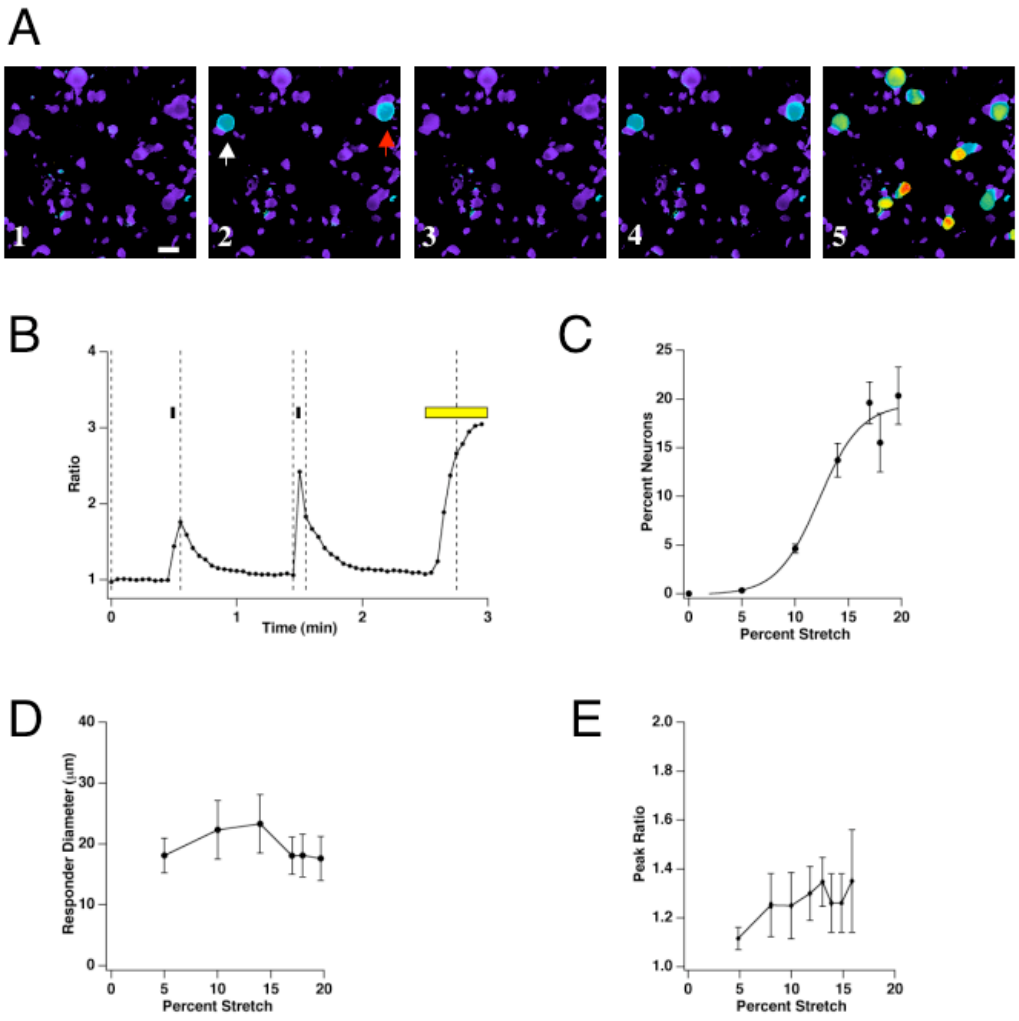
A
1
2
3
4
5
B
Ratio
Time (min)
C
Percent Neurons
Percent Stretch
D
Responder Diameter (μm)
Percent Stretch
E
Peak Ratio
Percent Stretch

Figure 10.

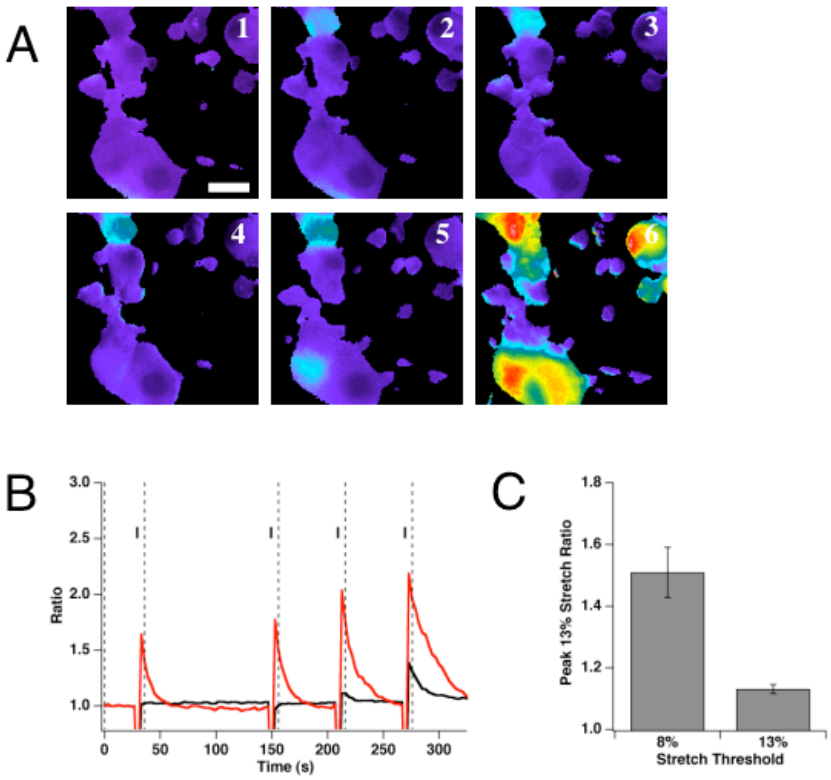
A
1
2
3
4
5
6
B
Ratio
3.0
2.5
2.0
1.5
1.0
0
50
100
150
200
250
300
Time (s)
C
Peak 13% Stretch Ratio
1.8
1.6
1.4
1.2
1.0
8%
13%
Stretch Threshold

Figure 11.

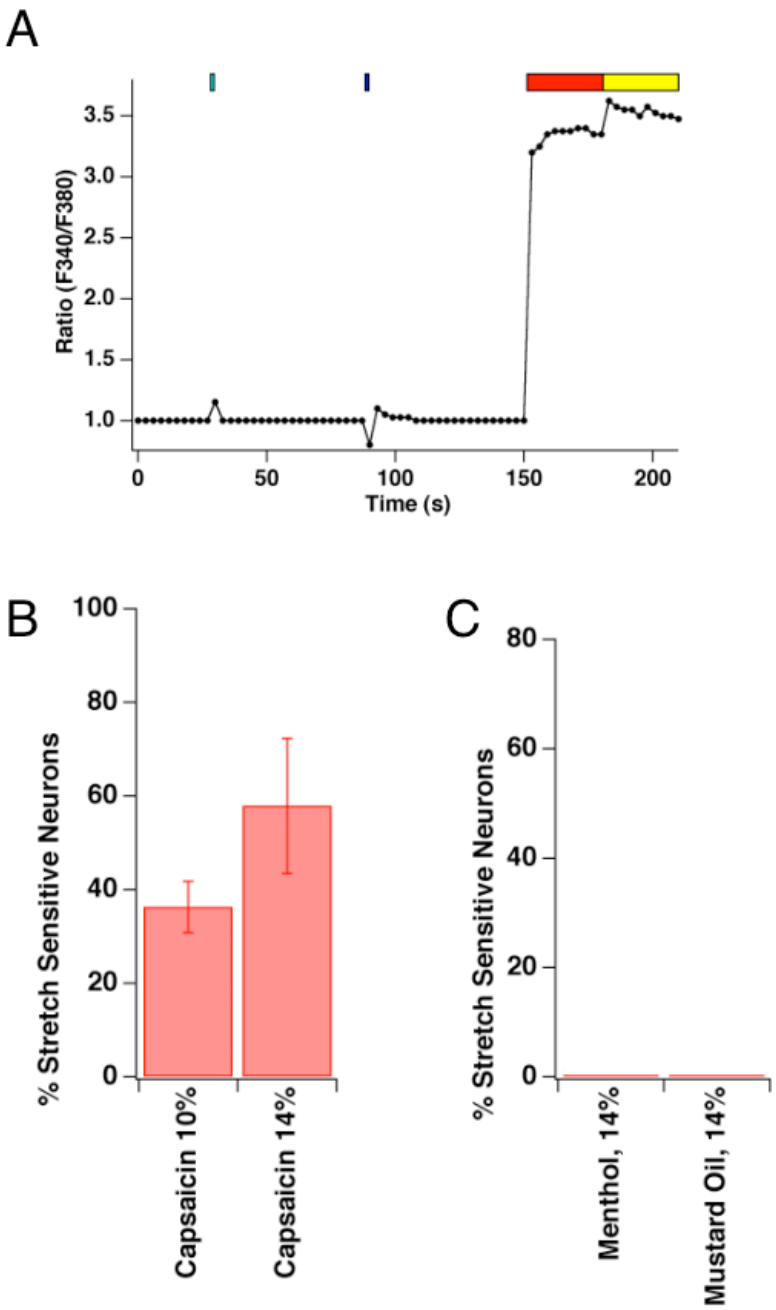
A
Ratio (F340/F380)
3.5
3.0
2.5
2.0
1.5
1.0
0
50
100
150
200
Time (s)
B
% Stretch Sensitive Neurons
100
80
60
40
20
0
Capsaicin 10%
Capsaicin 14%
C
% Stretch Sensitive Neurons
80
60
40
20
0
Menthol, 14%
Mustard Oil, 14%

Figure 12.

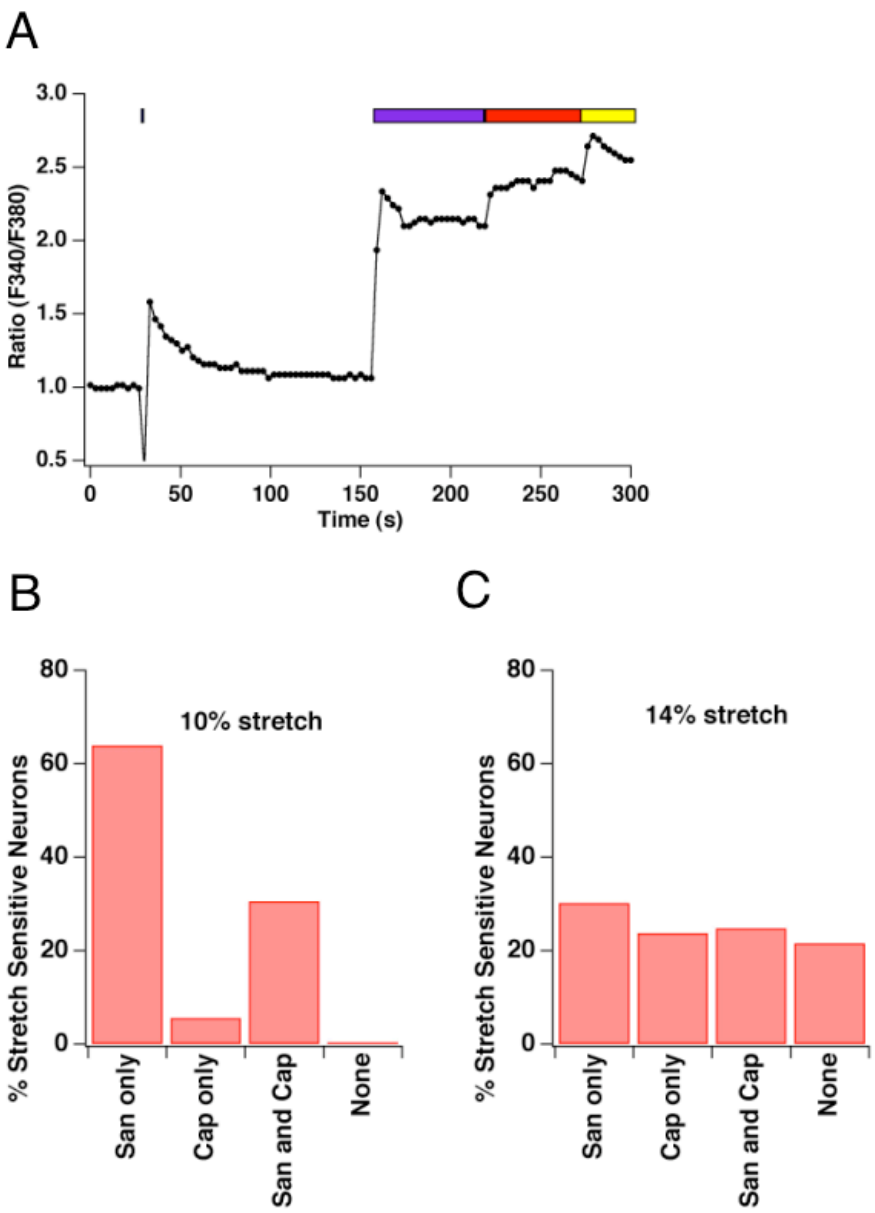
A
3.0
2.5
2.0
1.5
1.0
0.5
Ratio (F340/F380)
0
50
100
150
200
250
300
Time (s)
B
10% stretch
% Stretch Sensitive Neurons
80
60
40
20
0
San only
Cap only
San and Cap
None
C
14% stretch
% Stretch Sensitive Neurons
80
60
40
20
0
San only
Cap only
San and Cap
None

Figure 13.

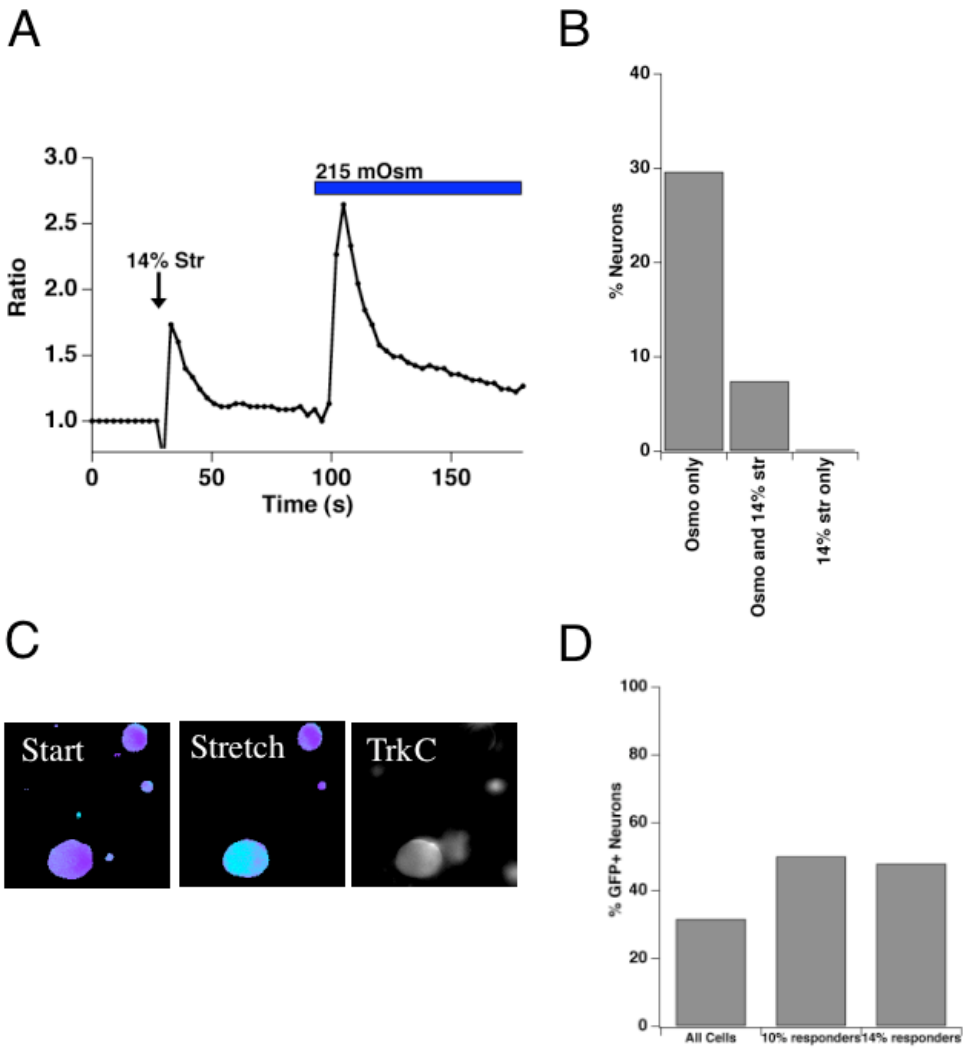
A
3.0
2.5
2.0
1.5
1.0
Ratio
215 mOsm
14% Str
0
50
100
150
Time (s)
B
40
30
20
10
0
% Neurons
Osmo only
Osmo and 14% str
14% str only
C
Start
Stretch
TrkC
D
100
80
60
40
20
0
% GFP+ Neurons
All Cells
10% responders
14% responders

Figure 14.

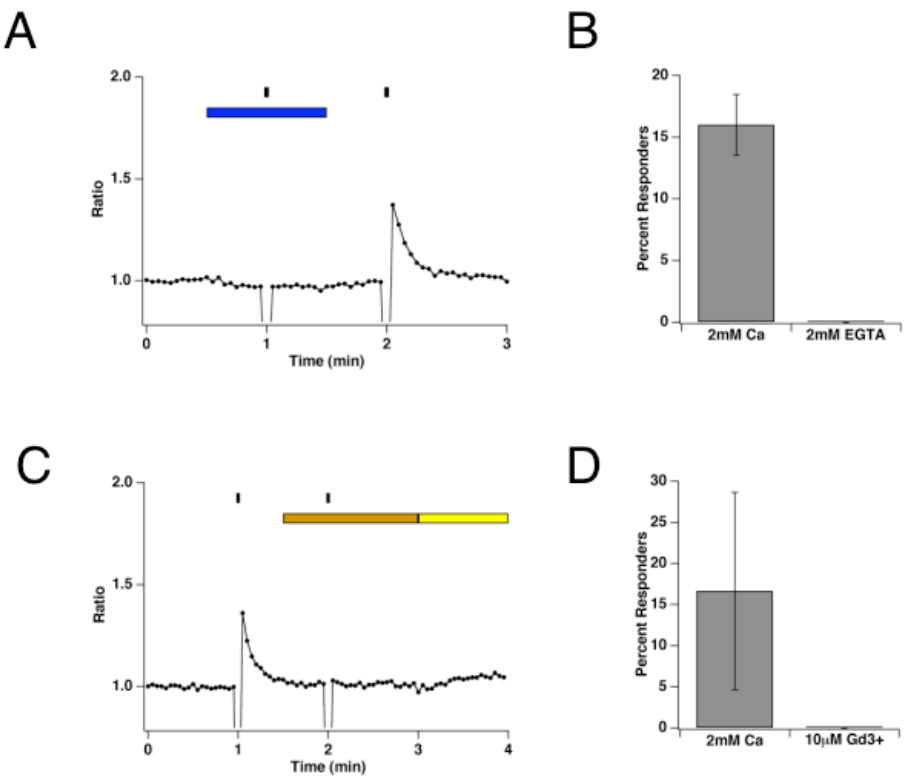
A
B
C
D
Ratio
Time (min)
Percent Responders
2mM Ca
2mM EGTA
10μM Gd3+

Figure 15.

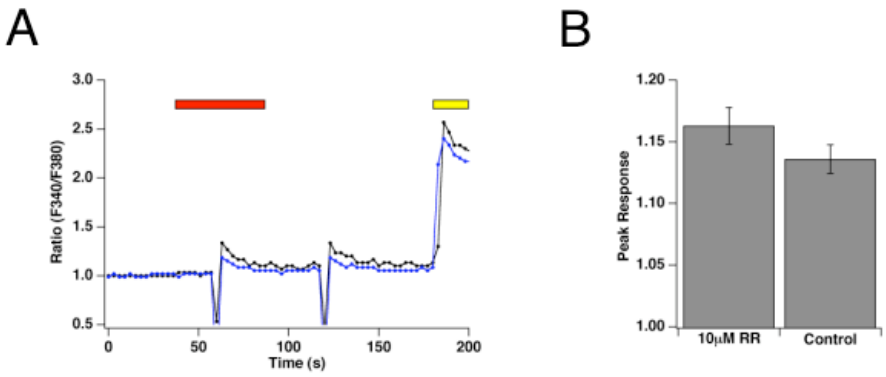

Figure 16.

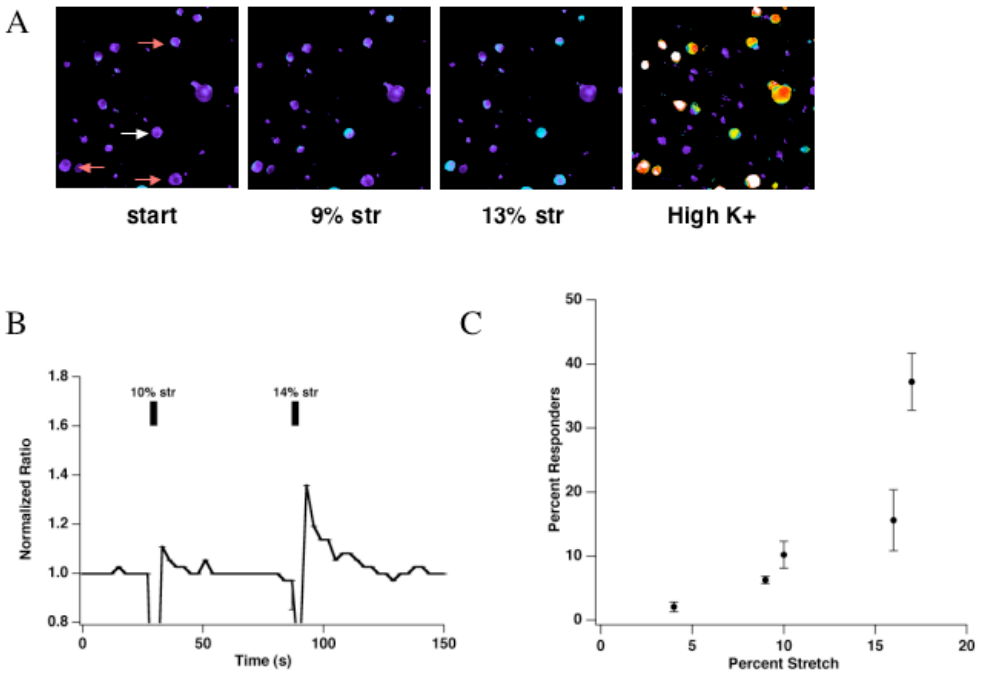
A
start
9% str
13% str
High K+
B
10% str
14% str
Normalized Ratio
1.8
1.6
1.4
1.2
1.0
0.8
0
50
100
150
Time (s)
C
Percent Responders
50
40
30
20
10
0
0
5
10
15
20
Percent Stretch

Figure 17.

A

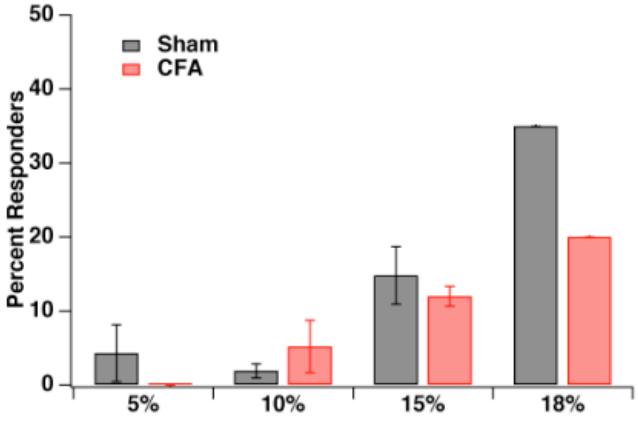
Sham
CFA
Percent Responders
50
40
30
20
10
0
5%
10%
15%
18%

B

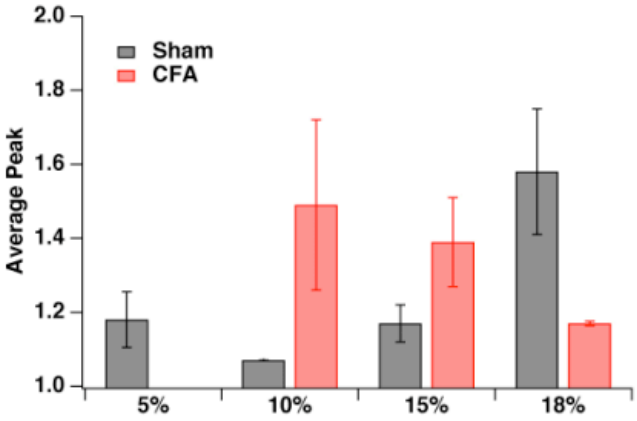
Sham
CFA
Average Peak
2.0
1.8
1.6
1.4
1.2
1.0
5%
10%
15%
18%

CHAPTER FOUR

EXPRESSION CLONING AND TOXIN INHIBITION SCREENS TO IDENTIFY NOVEL REGULATORS OF MECHANOTRANSDUCTION

Introduction

The study of mechanotransduction in mammals is at a critical juncture. Progress in understanding the mechanisms responsible for our senses of touch and hearing is stymied by the inability to identify the protein(s) responsible for causing depolarizing currents in sensory neurons and hair cells. While currents evoked by mechanical stimuli can be thoroughly characterized, we do not know what type of channel is activated.

Technical challenges abound in this area of research. First, somatosensory nerve endings are inaccessible both pharmacologically, due to the epidermal barrier, and electrically, due to their extremely small size. Mutations disrupting hair cell mechanotransduction cause these cells to degenerate, making the analysis of any putative channel mutants extremely difficult. Secondly, while sensory neurons and hair cells are the primary sensory transducers of mechanical stimuli, many other types of cells are mechanosensitive, making it problematic to take subtractive approaches to identifying unique proteins. Finally, unlike in vision and olfaction, where transduction components have been conserved from simpler organisms, channels thought to be mechanosensors in *Drosophila melanogaster*, *Caenorhabiditis elegans*, and *Danio rerio* have not been shown to be primary sensors in mouse. At least one of the proposed mechanotransduction channels, NOMP-C, has no mammalian counterpart. Novel unbiased approaches to identifying components are needed in order for the field of mammalian mechanosensation to advance.

Expression cloning techniques have been very successful in identifying receptors and ion channels mediating neuronal activation. For example, the identification of the capsaicin receptor TRPV1 was enabled by the detection of heterologously expressed

capsaicin-evoked channel activity in pools of a sensory neuron cDNA library (Caterina et al. 1997). Other chemical receptors, including the menthol receptor TRPM8 (McKemy et al. 2002) and the platelet ADP receptor P2Y12 (Hollopeter et al. 2001), were identified in similar expression cloning approaches.

Another strategy for discovering new molecules is to identify novel high-affinity agonists or antagonists of the response of interest. Venomous or poisonous organisms are a rich source of biologically active compounds with unknown molecular targets. Natural compounds identified from these toxic plants and animals have proven invaluable in the study of ion channels. The classic example of α-bungarotoxin illustrates how discovery of a novel high-affinity antagonist can lead to the identification of molecules. The demonstration that α-bungarotoxin bound irreversibly to acetylcholine receptors led to its subsequent radioactive labeling and to the biochemical isolation of the nicotinic acetylcholine receptor alpha subunit from the electric eel (Changeux et al. 1970). While such high affinity agonists are rare, novel agonists and antagonists with specificity for their targets can still reveal a great deal about structure and mechanism of a receptor.

The stretch assay described in previous chapters represents a technical advancement that enables the high-throughput screening of inhibitory compounds, cDNA libraries, and responses to gene knockdown using RNA interference. We have screened a sensory neuron cDNA library using both calcium imaging and FM 1-43 labeling, and we have also screened a collection of spider, scorpion, and cone snail venoms for activities on sensory neurons and inhibition of stretch responses in vascular smooth muscle cells. While we have yet to identify the mechanotransduction channel, these approaches

constitute new methods that can be expanded upon in the search for molecules mediating mechanotransduction.

Results

We first tested whether GsMTx4, a peptide from spider venom that is reported to block mechanosensitive channels (Suchyna et al. 2000), inhibited calcium entry during stretch. In rat aortic smooth muscle cells, incubation with a relatively high concentration of this peptide caused a small but significant decrease in intracellular calcium in response to stretch (Figure 18A). The kinetics and general shape of the response remained unaltered. The effect of this peptide could result from partial block of plasma membrane calcium-permeable channels or from inhibition of intracellular store release. We did not see effects of GsMTx4 on the percentage or magnitude of stretch responses in trigeminal sensory neurons (Figure 18B and 18C). We conclude that this peptide has little to no effect on stretch responses of these cells. Its effect on other cell types could be due to different mechanosensitive channels expressed in each cell type or to an effect on lipid-protein interaction that causes more pronounced effects in patch suction experiments than on whole cell stretch (Suchyna et al. 2004). Unfortunately, this peptide could not be used as a positive control for our stretch inhibition screen.

We tested a collection of 22 spider and scorpion venoms and 13 cone snail venoms against the stretch responses in smooth muscle cells. We identified seven crude venoms that significantly reduced stretch-activated calcium entry. Of these venoms, one was eliminated due to severe enzymatic activity and four others did not show block when retested. Of the two remaining venoms showing reproducible blocking activity, that from the *Physocyclus mexicanus* spider showed almost complete block of calcium entry

(Figure 19A). The IC_{50} of the crude venom is approximately a 1:1000 dilution of pure venom (Figure 19B). Importantly, the ionomycin response was not altered, even at concentrations 10-fold over the IC_{50}. We conclude that this venom is affecting a cellular component necessary for stretch-induced activation of smooth muscle cells.

To identify the component of this venom responsible for its blocking ability, we fractionated the venom by reversed phase HPLC. The resulting chromatogram (Figure 19C) illustrates that this venom has many molecular species that can be separated by hydrophobicity. We collected 1ml fractions and assayed them using the stretch system. While a few of these fractions showed partial block, none were able to duplicate the effects of the crude venom. We recombined all of the fractions isolated by HPLC and tested this mixture side by side with the crude venom, but this failed to cause block.

In studying the crude venom, we observed that cells changed shape slightly after application of the crude venom and that this effect was concentration dependent. The apparent detaching of portions of cells from the membrane could indicate that an enzymatic activity in the venom is affecting integrins or other adhesion molecules required for cells to respond to stretch. Consistent with this interpretation, we found that components of the crude venom less than 10 kiloDaltons did not cause block while components larger than 10kD produced block (data not shown). Furthermore, the enzymatic activity did not reproducibly fractionate by HPLC, an expected result if a molecule is too large to travel linearly in the HPLC gradient. While we do not know the molecular identities of affected plasma membrane components, we suspect that adhesion molecules play a large role in stretch activation of all cell types and that disturbing their function would necessarily reduce mechanosensitive channel activation.

In the process of screening this collection of venoms, we identified a subset that caused intracellular calcium influx independent of mechanical stimulation in subpopulations of trigeminal sensory neurons (Figure 20 and Figure 21). These venoms represent sources of new agonists that could aid in defining subpopulations of sensory neurons and studying pain mechanisms.

Stings by the scorpion *V. spinigerus*, a native of the southwest United States and northern Mexico, causes transient pain and swelling in the area of contact and can be lethal to small animals. Crude venom from this scorpion causes dramatic oscillations in systemic arterial pressure when administered to cats (Russell et al. 1968). We find that *V. spinigerus* venom causes excitation in 60-70% of sensory neurons (Figure 20). Interestingly, application of this venom causes both immediate calcium rise in neurons and delayed calcium rise in non-neuronal populations. We studied the overlap between venom activation and that of capsaicin and sanshool, agonists that activate defined subpopulations of sensory neurons. *V. spinigerus* venom excites just under 80% of capsaicin-sensitive neurons but only 50% of sanshool-positive neurons. Furthermore, a large portion of venom-sensitive neurons were not capsaicin or sanshool sensitive (Figure 20C). The significant but incomplete overlap with capsaicin suggests that V. spinigerus venom directly activates nociceptors in a TRPV1-independent manner, causing its painful sting. This mechanism is distinct from that of the recently identified vanillotoxins from the spider *P. cambridgei* that activate TRPV1 to cause pain (Siemens et al. 2006). Further analysis by HPLC fractionation and activity on other cell types should yield interesting insights into how this organism causes pain.

Other venoms tested initiate calcium rise in larger subsets of neurons. The venom of *Hadrurus arizonensis*, another scorpion from the southwestern U.S., activates 88% of trigeminal neurons (Figure 21). While little is known about the venom from this particular species, other scorpions from the genus *Hadrurus* produce toxins capable of blocking potassium currents through the Shaker channel (Schwartz et al. 2006). Block of a K+ channel can lead to depolarization and activation of voltage-gated calcium channels, leading to calcium influx. Therefore, the observed increase in intracellular calcium is likely because the venom of *H. arizonensis* contains similar compounds acting in an analogous fashion to those of related species.

To summarize our venom screening data, we have uncovered multiple venoms with a range of effects on sensory neurons and smooth muscle cells. We have identified two venoms that cause significant block of stretch-activated calcium rise in vascular smooth muscle. The effect of the stronger of these two venoms may be due to enzymatic activities existing in the crude preparation, while the other has yet to be studied thoroughly. In addition, we discovered novel activities in two crude venom preparations from scorpions. These studies are in their infancy and many directions exist for future work. For example, fractionation and testing of components of the latter scorpion venoms could uncover new mechanisms by which pain signals are transduced.

In addition to employing venoms to ask questions about the mechanisms of mechanotransduction and pain, we have attempted forward genetic screens to identify new players in sensory neuron touch transduction. We chose to screen using a 14% stretch stimulus given that our sensory neuron dose-response reaches near-saturation at this level. We did two parallel screens using different detection methods. One screen

relied on the uptake of FM 1-43 in response to transient stretch. The second screen used calcium imaging to detect real-time responses of cells to stretch. In both cases, we transfected pools of a previously constructed cDNA library from DRG neurons into HEK293T cells.

We first verified that FM1-43 uptake by transfected cells could be used to reliably identify cells containing specific cDNAs. To test this, we transfected a pool of 12,000 cDNAs known to contain the capsaicin receptor TRPV1 into HEK cells and applied FM 1-43 in the presence or absence of capsaicin. We observed dye loading in a few cells in each 10x field of view only in capsaicin-treated cells (Figure 22A). These cells often appeared in clusters, suggesting that a single TRPV1-transfected cell had recently divided.

We screened 720,000 independent cDNA clones with FM 1-43 and 14% stretch, using FM 1-43 without stretch as a negative control. We used a vacuum-sealed plate that stretched 24 wells at once to increase throughput, and images were acquired after washing out excess dye. We identified a small number of stretched pools containing significant labeling over unstretched controls (Figure 22B). Attempts to follow this labeling activity in smaller subpools revealed clusters of cells labeling with dye (bottom panels). Unfortunately, we also observed an increased FM 1-43 background labeling in unstretched controls when pools contained less than 1000 cDNAs. This complicated efforts to follow positive signals.

We decided to take a separate approach by screening the same library using real-time calcium imaging during stretch. This screen would eliminate the background fluorescence problems caused by FM 1-43 as well as allow calcium signals to be

temporally correlated with stretch stimulation. However, it is significantly more time intensive since live imaging must be done for each trial individually. We identified multiple cDNA pools that showed at least one cell responding to stretch by cytoplasmic calcium increases (Figure 22C). Three of these pools were further analyzed by subpooling but were ultimately eliminated as false positives resulting from prior mechanical stimulus while loading membranes into the StageFlexer. Although other cell types such as smooth muscle cells do not appear to be sensitive to the perturbations of setting up the system, library-transfected HEK cells may be in a more fragile state due to their overexpression of many proteins and thus may be more likely to become preactivated with a small stimulus. It is possible that more positive pools could be uncovered if this prestimulation had caused desensitization of transfected mechanosensitive channels, and it will be worthwhile to repeat this analysis with new methods we have recently developed to minimize mechanical perturbations prior to imaging.

Discussion

The technology we have utilized to mechanically stimulate cells with stretch has enabled the design of multiple types of screens to detect novel molecules or inhibitors of the stretch response. In particular, we have used cell types shown to be stretch sensitive and exploited advantages of non-neuronal cell types for screening purposes. Smooth muscle cells have great promise as an assay system for mechanotransduction because of the relative uniformity of their responses and their ability to label with dyes in an activity-dependent manner. In addition to screening small molecules like venom-derived peptides and chemical libraries for their ability to inhibit stretch-evoked calcium entry,

techniques such as RNA interference can be used in this system that could not be used in sensory neurons. In collaboration with other lab members, we are currently designing a higher throughput stretch assay in a line of human vascular smooth muscle cells that could be used to screen libraries of small inhibitory RNAs.

Expression cloning approaches can be extremely powerful because molecules conferring an activity can be identified based on their function in a cellular context without needing any other information about the protein. However, the major limitation in expression cloning is the necessity for a single protein to be able to reconstitute the cellular activity. While many chemical receptors have been identified using this approach, the molecules transducing mechanical stimuli may be more complex. Indeed, in *C. elegans*, at least three channel subunits have been identified that contribute to the mechanotransduction current (Huang et al. 1994; O'Hagan et al. 2005). In addition, the correct accessory subunits linking the channel to matrices inside and outside the cell are critical to exert force on the channel (Goodman et al. 2002). To reconstitute this system has proven challenging for the worm mechanotransduction field and is likely at least as difficult in mammalian cells. Recently, a knockout in the mammalian protein SLP3, a mammalian homologue of the C. elegans intracellular linker MEC-2, has been shown to cause alterations in touch-induced behaviors (Wetzel et al. 2007). It may be necessary to express this protein along with candidate mechanotransduction channels in order to reconstitute a mechanically sensitive mammalian cell.

The exploitation of stretch as a high throughput screening technique is in its early stages. Additional screening approaches using RNA interference, chemical genetics, or known numbing agents may be useful in finding specific blockers of

mechanotransduction. Furthermore, new methods to permanently mark activated cells are being developed, such as NFAT-dependent luciferase transcription (Graef et al. 1999), and these may be employed rather than FM 1-43 loading to mark responding cells. We look forward to the next generation of screens using stretch and believe that this system will be crucial in identifying the elusive molecules responsible for mammalian mechanotransduction.

Figure Legends

Figure 18. The peptide GsMTx4 has limited effects on stretch responses in smooth muscle or sensory neurons. A, Average trace of rat aortic smooth muscle cells responding to 14% stretch (blue bar) and ionomycin (yellow bar). Black trace, control (n=49); red trace, 10μM GsMTx4 (n=77) before (5min) and during experiment. B, Two stretch responsive trigeminal sensory neurons. Blue box, 14% stretch. Black trace, control; red trace, 10μM GsMTx4 before (5min) and during experiment. Spike at 90s is application of high potassium. C, Percent and average peak of stretch-sensitive trigeminal sensory neurons with and without incubation in GsMTx4.

Figure 19. *Physocyclus mexicanus* venom inhibits stretch activation of smooth muscle cells. A, Average responses of control and venom-treated cells shown in A. Venom was used at a 1:100 dilution of the crude venom. Blue bar, 14% stretch. Yellow bar, 10μM ionomycin in 10mM calcium. B, Dose-response of crude venom on inhibition of stretch-activated calcium influx. IC_{50} = 1:1000 dilution for crude venom and was calculated by fitting a sigmoidal curve to the data. Error bars are SEM. C, Chromatogram of *Physocyclus mexicanus* venom as determined by RP-HPLC.

Figure 20. *Vejovis spinigerus* crude venom activates a population of sensory neurons. A, still frames of a time lapse experiment showing response to crude venom application for 4 or 32 seconds, followed by high potassium. Note that initially the toxin activates large diameter sensory neurons, and with a longer incubation other non-neuronal cells become

activated. B, example trace of two neurons responding to crude venom (orange bar), one of which is also sensitive to capsaicin (red bar). C, percentage of neurons responding to crude venom and/or capsaicin or sanshool. Data are compilations of 2-3 independent trials.

Figure 21. *Hadrurus arizonensis* crude venom activates 90% of sensory neurons. A, still frames of a time lapse experiment showing response to crude venom application for 4 or 40 seconds, followed by high potassium. B, example trace of two neurons responding to crude venom (orange bar), one of which is also sensitive to sanshool (blue bar). Yellow bar, high potassium. C, percentage of neurons responding to crude venom and/or capsaicin or sanshool. Data are compilations of 2-3 independent trials.

Figure 22. Expression cloning reveals pools of cDNA that may contain mechanosensitive channels. A, DRG library pool of 12,000 cDNAs known to contain TRPV1 was expressed in HEK293T cells and incubated with 10μM TRPV1 in the presence (top) or absence (bottom) of 1μM capsaicin for 30 seconds. Left images are brightfield images of the transfected cells; right images are fluorescence pictures of FM 1-43 labeling in the same cells. All images are at 10x magnification. Note that the expected detection rate of one gene expressed in a pool is approximately 5 cells in a 10x field of view. B, Sample results of an expression cloning screen using FM 1-43 labeling to detect stretch-activated cells. In each case, 1μg of plasmid DNA or library DNA was transfected. Top panels, pCDNA3 expression with and without stretch stimulation. Middle panels, a pool of 12,000 cDNAs containing cells that show stretch-specific FM 1-

43 labeling in a few cells. Bottom panels, subpool of 4,000 cDNAs from the above pool of 12,000. Clusters of positive cells were observed in many subpools that were subjected to stretch. C, Sample results of an expression cloning screen using calcium imaging to detect stretch-activated cells. Top panels, pCDNA3 expression with and without stretch stimulation. Bottom panels, pool of 10,000 cDNAs from rat smooth muscle cells showing a single cell responding to 14% stretch (arrow). Stretched images are approximately 4 seconds after the release of stretch.

Figure 18.

A

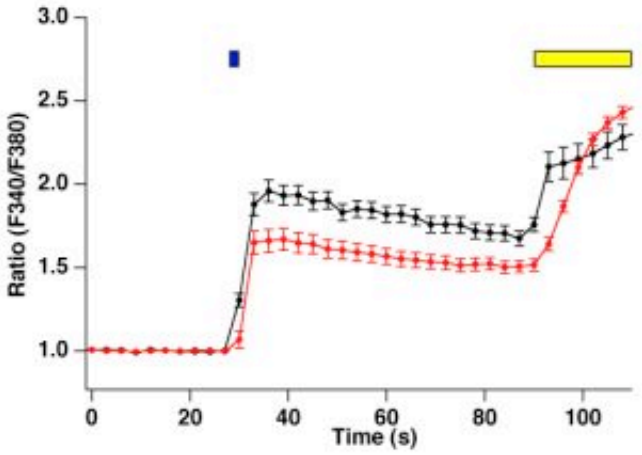

B

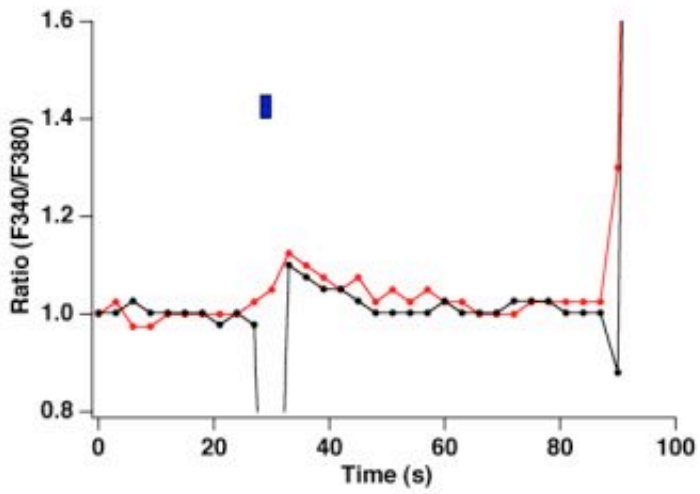

C

	Percent Responders	Peak Response
Control	8.7 (6/69)	1.09 +/- 0.01
GsmTx4	11.3 (6/53)	1.12 +/- 0.05

Figure 19.

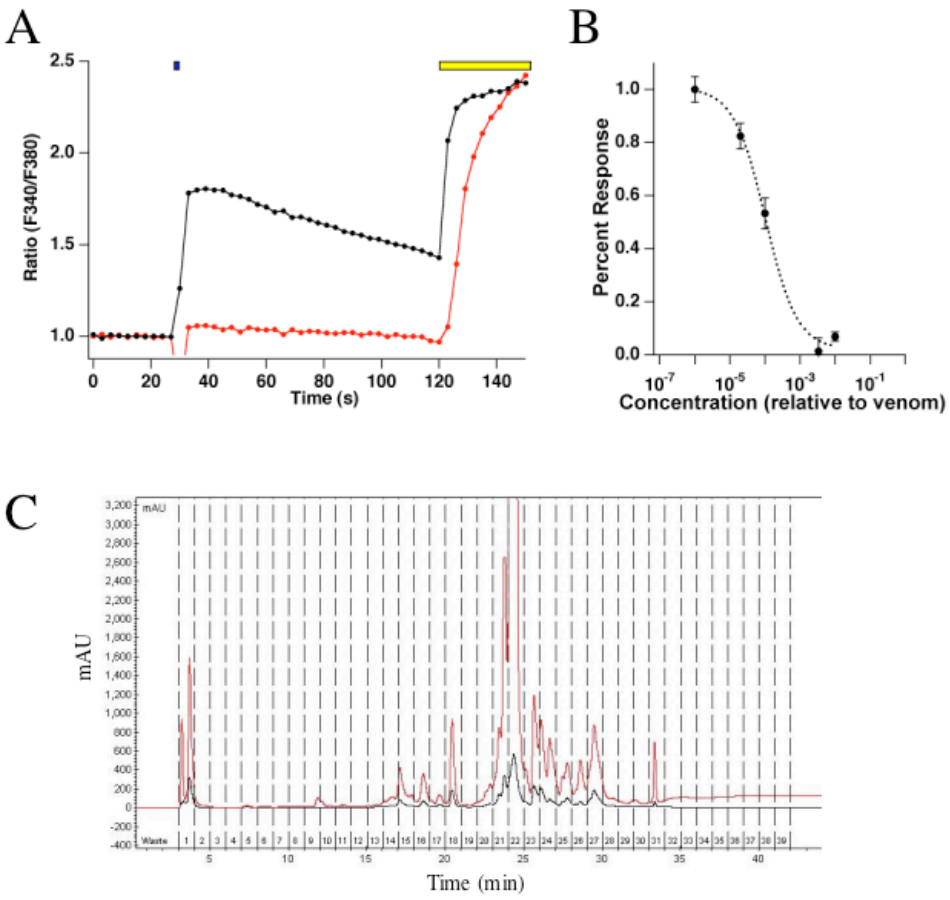
A
Ratio (F340/F380)
Time (s)
B
Percent Response
Concentration (relative to venom)
C
mAU
Time (min)

Figure 20.

A

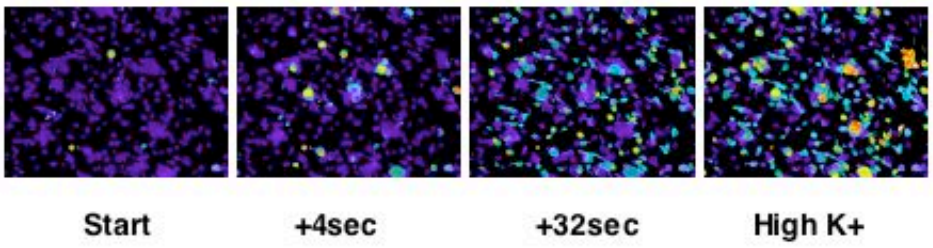

B

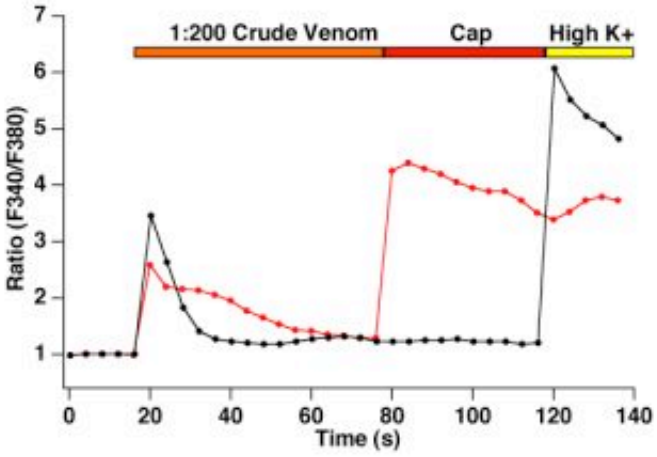

C

Venom only	30.4 (28/92)	Venom only	45.1 (23/51)
Venom + Cap	38 (35/92)	Venom + Sanshool	19.6 (10/51)
Cap only	10.9 (10/92)	Sanshool only	19.6 (10/51)
No Response	20.7 (19/92)	No Response	15.7 (8/51)

Figure 21.

A

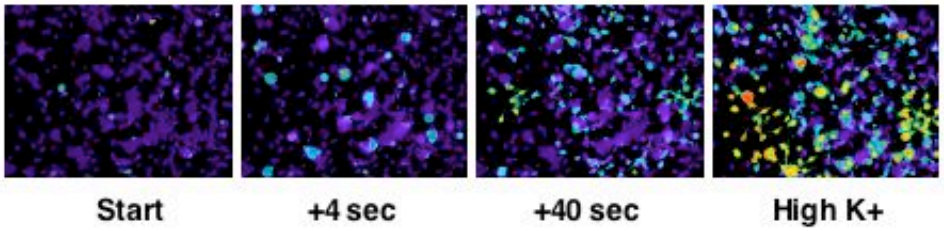

B

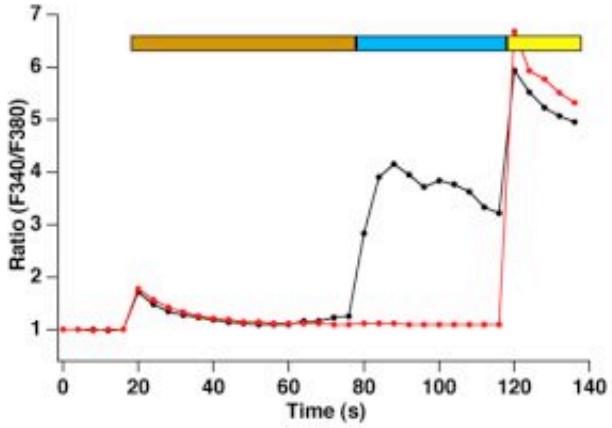

C

Venom only	37.5 (9/24)	Venom only	34.1 (15/44)
Venom + Cap	50 (12/24)	Venom + Sanshool	54.5 (24/44)
Cap only	4.2 (1/24)	Sanshool only	4.5 (2/44)
No Response	8.3 (2/24)	No Response	6.9 (3/44)

Figure 22.

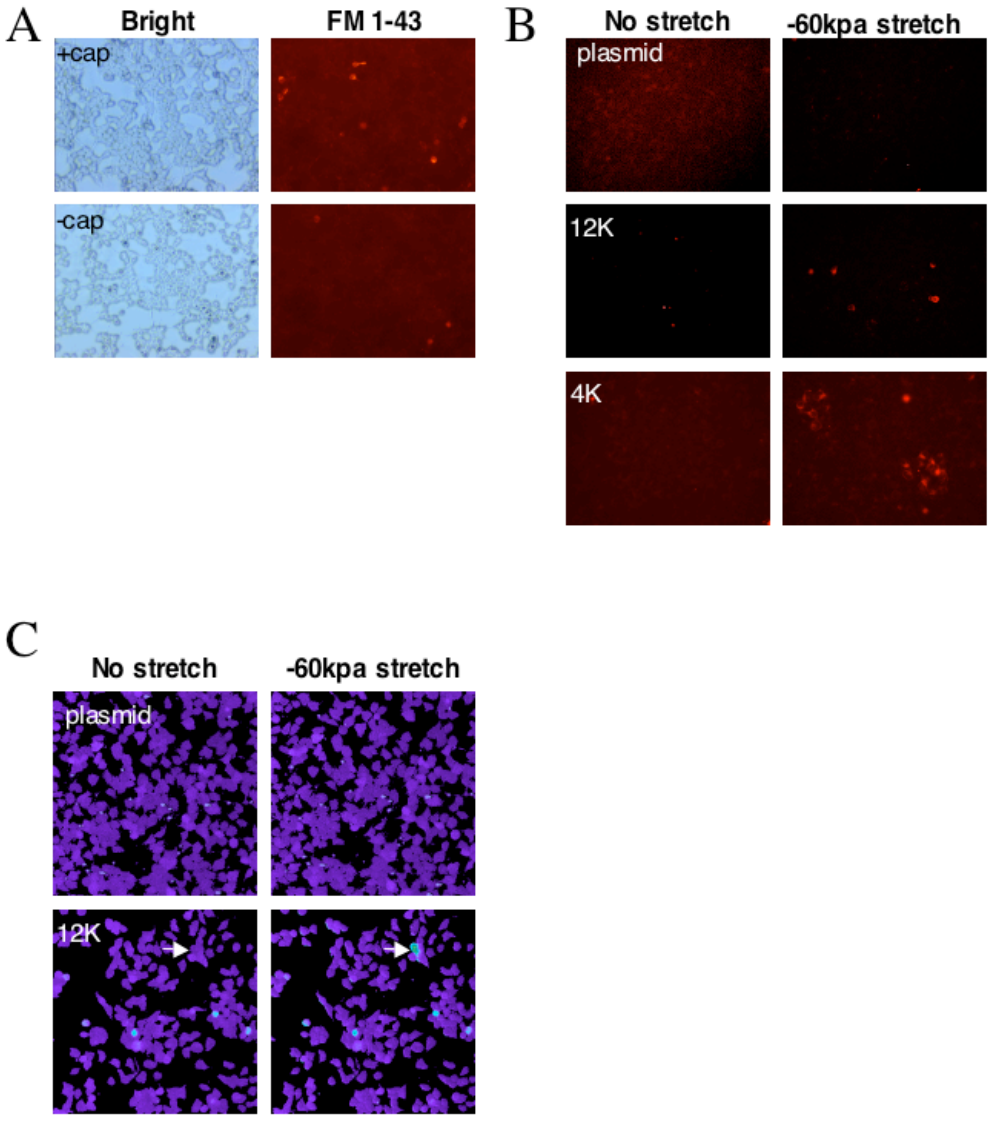
A
Bright
FM 1-43
+cap
-cap
B
No stretch
-60kpa stretch
plasmid
12K
4K
C
No stretch
-60kpa stretch
plasmid
12K

DISCUSSION AND FUTURE DIRECTIONS

Mechanotransduction is a ubiquitous stimulus to virtually all cells, whether they reside on the surface of the skin or on the interior of blood vessels. A multitude of physiological processes depend critically on the proper sensing of forces, such as hearing, proprioception, intestinal contraction, cardiac pumping, lung expansion and contraction, and touch sensation. The discovery of the molecules responsible for mechanotransduction will have tremendous applications to science and medicine. Progress in this field waits for the advent of new technologies to mechanically stimulate cells, record from tiny nerve endings, and reconstitute channels in vitro. In addition, methods need to be developed to mark responding cells, sort heterogeneous populations, and define primary versus secondary detectors. We have made forward progress in this field by employing an underappreciated stretch stimulation technique in combination with live imaging of intracellular calcium to demonstrate the first use of a multi-cell mechanical stimulus which can be easily adapted to screen for stretch-sensitive ion channels.

Stretch activation of ion channels, in contrast with activation by suction, poking, or osmotic swelling, may depend on additional parameters due to the requirement for tight adhesion to the stretched silicone membrane. In smooth muscle cells, integrin activation is sufficient to trigger L-type calcium channel activation in vascular smooth muscle and subsequent vasoconstriction (Wu et al. 1998; Wu et al. 2001; Waitkus-Edwards et al. 2002), suggesting that this could be one mechanism of stretch sensing. Stretch-activated ion channels in smooth muscle can also be activated independently of integrins (Wu et al. 2001). We are likely enabling both of these mechanisms with our stretch assay due to the adhesion of smooth muscle cells to the surface of the silicone

membrane using the integrin substrate fibronectin. Somewhat perplexingly, we are unable to observe activation of voltage-gated calcium channels by high potassium solutions under the same conditions that we can see robust stretch activated calcium entry. Because de-differentiation of smooth muscle cells occurs in culture, the cells used in our stretch experiments have likely lost expression of voltage-gated calcium channels. At least some subtypes of voltage-gated calcium channels do not seem to be involved in mechanosensation by somatosensory neurons (Gotoh et al. 1999).

Our results showing stretch-activated calcium entry in smooth muscle cells and FM 1-43 loading in these cells is significant in that it enables screens not possible in neurons due to their heterogeneity. While we do not know if the channels responsible for mechanosensation in neurons and smooth muscle are identical, we have shown that both cell types rely on calcium entry across the plasma membrane using mechanisms sensitive to known channel-blocking agents. Using this system, loss-of-function screens that were not possible with single-cell methods can now be attempted with chemical inhibitors or RNA interference.

With respect to the identity of the transduction channels, two pieces of evidence suggest that smooth muscle and sensory neurons could use different mechanisms. First, smooth muscle cells label with FM 1-43 dye when stretched, but neurons do not. Second, smooth muscle cell stretch responses are sensitive to ruthenium red, while similar concentrations do not affect neuronal responses. Although these observations do not constitute definitive evidence for two divergent transduction mechanisms, they suggest that differences exist between these cell types' responses to stretch on a cellular level.

In the vascular system, stretch is the most representative in vitro stimulus we can employ to mimic forces felt in blood vessels during systole. In this phase of the cardiovascular cycle, the aorta receives a bolus of blood pumped from the heart and its walls are put under significant circumferential pressure. Endothelial cells lining the interior of the vessel are put under strain, and the smooth muscle tissue surrounding it is subjected to this same force. A multitude of studies have investigated the relationships between mechanical force due to stretch and induction of gene expression that can lead to long-term changes in blood vessel pliancy (Birukov et al. 1995; Kolpakov et al. 1995). In addition, calcium influx is required for the myogenic response that occurs in healthy blood vessels due to increased arteriolar pressure (Hill et al. 2001). The initiation events leading to these responses remain a black box. These earlier studies have used the same stretch stimulus that we have used but applied a continuous sinusoidal stretch. To fill in the gap between stimulus and cellular changes, we have imaged cells during their first response to stretch. Our results are in agreement with evidence from smooth muscle cells using other types of mechanical stimuli and argue that mechanosensitive ion channels contribute to intracellular calcium rise, which then initiates cellular contraction and the myogenic response. Using this cell type as a simplified model, we can potentially learn both about mechanisms regulating arteriolar pressure and also use loss-of-function approaches to uncover global principles of mammalian mechanotransduction.

Because we do not know if the mechanisms underlying force sensing are in different physiological processes are conserved, we have also approached this problem in the somatosensory system using primary cultures of neuronal cell bodies from the trigeminal and dorsal root ganglia, the principal detectors of touch. Stretch represents a

new stimulus applied to the study of mechanotransduction in neurons. It is less clear in sensory neurons than in smooth muscle cells whether stretch is the most relevant type of mechanical stimulus; we have admittedly taken a step away from the anatomical organization of this system by culturing only the cell bodies and in the process cutting the endogenous nerve endings. A combinatorial approach with a range of techniques is appropriate for this system and should yield many insights into the biology and coding of mechanosensory inputs. In particular, studies using the skin-nerve prep can give information about detection at the nerve endings in a relatively unaltered context, while studies of cell bodies can reveal information about the types of currents induced and their pharmacology.

One vexing question requiring further study is why different percentages of sensory neurons respond to mechanical forces applied in different ways. Careful mathematical analyses of the forces applied to cells using varied stimulus types could begin to answer this question. We observe that 20% of neurons respond to large amounts of stretch. Within this population we see both low-threshold Aβ neurons, as marked by Trk-C expression, and nociceptive C-fiber neurons, as marked by capsaicin sensitivity. These results indicate that the range of stimulus magnitudes used in our studies is sufficiently wide and that large stretches surpass even high neuronal activation thresholds. A definitive answer to this conundrum awaits identification of the sensor(s) required in sensory neurons.

While some mammalian channels have been suggested to be responsive to non-osmotic mechanical stimuli, such as members of the K2P (Maingret et al. 1999), definitive analysis awaits the ability to reconstitute this system. The bacterial channel

MscL is the sole channel for which this has been achieved in a cell-free system (Sukharev et al. 1994). Techniques such as reconstitution of channels into vesicles or planar lipid bilayers will be necessary to demonstrate if any eukaryotic channels can be gated by membrane stretch in the absence of linker molecules. In heterologous expression systems, mechanosensitivity cannot be demonstrated for candidate channels such as ASIC2, ASIC3, and TRPA1. While these particular candidates have no mechanosensation phenotypes when knocked out (Drew et al. 2004; Roza et al. 2004; Bautista et al. 2006), candidates that pass loss-of-function tests will need to be confirmed using some other method if they are to be considered direct sensors rather than downstream effectors.

In summary, we have applied new mechanical stimulation techniques in conjunction with real-time imaging to detect initial mechanotransduction events in neuronal and non-neuronal mammalian cell types. This technique allows us for the first time to visualize somatosensory mechanotransduction, and it enables many types of gain- and loss-of-function screens that would not otherwise have been possible. Furthermore, it represents a higher-throughput way to analyze heterogeneous populations of cells from organs with diverse cellular compositions. This advance is most clearly realized in our study of stretch activation of peripheral sensory neurons, allowing the description of cell types with different mechanical thresholds. This technique has profound application in studies of many types of mechanosensitive cells and in the future should be extended to the cellular analysis of other mechanosensitive systems. Our demonstration of the ability to witness receptor potentials using calcium imaging has illuminated the transduction process that leads to action potentials in sensory neurons and contractile responses in

muscle cells. These studies have laid the groundwork for many future advances in the field of mechanosensation.

REFERENCES

Anishkin, A. and C. Kung (2005). "Microbial mechanosensation." Curr Opin Neurobiol **15**(4): 397-405.

Banes, A. J., J. Gilbert, et al. (1985). "A new vacuum-operated stress-providing instrument that applies static or variable duration cyclic tension or compression to cells in vitro." J Cell Sci **75**: 35-42.

Bautista, D. M., S. E. Jordt, et al. (2006). "TRPA1 mediates the inflammatory actions of environmental irritants and proalgesic agents." Cell **124**(6): 1269-82.

Beech, D. J. (2005). "Emerging functions of 10 types of TRP cationic channel in vascular smooth muscle." Clin Exp Pharmacol Physiol **32**(8): 597-603.

Bernardi, P., V. Paradisi, et al. (1984). "Pathway for uncoupler-induced calcium efflux in rat liver mitochondria: inhibition by ruthenium red." Biochemistry **23**(8): 1645-51.

Birukov, K. G., V. P. Shirinsky, et al. (1995). "Stretch affects phenotype and proliferation of vascular smooth muscle cells." Mol Cell Biochem **144**(2): 131-9.

Breese, N. M., A. C. George, et al. (2005). "Peripheral inflammation selectively increases TRPV1 function in IB4-positive sensory neurons from adult mouse." Pain **115**(1-2): 37-49.

Bryant, B. P. and I. Mezine (1999). "Alkylamides that produce tingling paresthesia activate tactile and thermal trigeminal neurons." Brain Res **842**(2): 452-60.

Caprini, M., A. Gomis, et al. (2003). "GAP43 stimulates inositol trisphosphate-mediated calcium release in response to hypotonicity." Embo J **22**(12): 3004-14.

Caterina, M. J., M. A. Schumacher, et al. (1997). "The capsaicin receptor: a heat-activated ion channel in the pain pathway." Nature **389**(6653): 816-24.

Chalfie, M. and M. Au (1989). "Genetic control of differentiation of the Caenorhabditis elegans touch receptor neurons." Science **243**(4894 Pt 1): 1027-33.

Changeux, J. P., M. Kasai, et al. (1970). "Use of a snake venom toxin to characterize the cholinergic receptor protein." Proc Natl Acad Sci U S A **67**(3): 1241-7.

Cho, H., J. Y. Koo, et al. (2006). "A novel mechanosensitive channel identified in sensory neurons." Eur J Neurosci **23**(10): 2543-50.

Cho, H., J. Shin, et al. (2002). "Mechanosensitive ion channels in cultured sensory neurons of neonatal rats." J Neurosci **22**(4): 1238-47.

Chuang, H. H., E. D. Prescott, et al. (2001). "Bradykinin and nerve growth factor release the capsaicin receptor from PtdIns(4,5)P2-mediated inhibition." Nature **411**(6840): 957-62.

Cibulsky, S. M. and W. A. Sather (1999). "Block by ruthenium red of cloned neuronal voltage-gated calcium channels." J Pharmacol Exp Ther **289**(3): 1447-53.

Cockayne, D. A., S. G. Hamilton, et al. (2000). "Urinary bladder hyporeflexia and reduced pain-related behaviour in P2X3-deficient mice." Nature **407**(6807): 1011-5.

Corey, D. P., J. Garcia-Anoveros, et al. (2004). "TRPA1 is a candidate for the mechanosensitive transduction channel of vertebrate hair cells." Nature **432**(7018): 723-30.

Corey, D. P. and A. J. Hudspeth (1979). "Ionic basis of the receptor potential in a vertebrate hair cell." Nature **281**(5733): 675-7.

Corey, D. P. and A. J. Hudspeth (1983). "Kinetics of the receptor current in bullfrog saccular hair cells." J Neurosci **3**(5): 962-76.

Davis, M. J., G. A. Meininger, et al. (1992). "Stretch-induced increases in intracellular calcium of isolated vascular smooth muscle cells." Am J Physiol **263**(4 Pt 2): H1292-9.

Drew, L. J., D. K. Rohrer, et al. (2004). "Acid-sensing ion channels ASIC2 and ASIC3 do not contribute to mechanically activated currents in mammalian sensory neurones." J Physiol **556**(Pt 3): 691-710.

Drew, L. J. and J. N. Wood (2007). "FM1-43 is a permeant blocker of mechanosensitive ion channels in sensory neurons and inhibits behavioural responses to mechanical stimuli." Mol Pain **3**: 1.

Drew, L. J., J. N. Wood, et al. (2002). "Distinct mechanosensitive properties of capsaicin-sensitive and -insensitive sensory neurons." J Neurosci **22**(12): RC228.

Drummond, H. A., M. J. Welsh, et al. (2001). "ENaC subunits are molecular components of the arterial baroreceptor complex." Ann N Y Acad Sci **940**: 42-7.

Funfschilling, U., Y. G. Ng, et al. (2004). "TrkC kinase expression in distinct subsets of cutaneous trigeminal innervation and nonneuronal cells." J Comp Neurol **480**(4): 392-414.

Gale, J. E., W. Marcotti, et al. (2001). "FM1-43 dye behaves as a permeant blocker of the hair-cell mechanotransducer channel." J Neurosci **21**(18): 7013-25.

Garcia-Anoveros, J., T. A. Samad, et al. (2001). "Transport and localization of the DEG/ENaC ion channel BNaC1alpha to peripheral mechanosensory terminals of dorsal root ganglia neurons." J Neurosci **21**(8): 2678-86.

Garry, E. M., A. Delaney, et al. (2005). "Varicella zoster virus induces neuropathic changes in rat dorsal root ganglia and behavioral reflex sensitisation that is

attenuated by gabapentin or sodium channel blocking drugs." Pain **118**(1-2): 97-111.

Goodman, M. B., G. G. Ernstrom, et al. (2002). "MEC-2 regulates C. elegans DEG/ENaC channels needed for mechanosensation." Nature **415**(6875): 1039-42.

Gotoh, H. and A. Takahashi (1999). "Mechanical stimuli induce intracellular calcium response in a subpopulation of cultured rat sensory neurons." Neuroscience **92**(4): 1323-9.

Graef, I. A., P. G. Mermelstein, et al. (1999). "L-type calcium channels and GSK-3 regulate the activity of NF-ATc4 in hippocampal neurons." Nature **401**(6754): 703-8.

Hayakawa, K., N. Sato, et al. (2001). "Dynamic reorientation of cultured cells and stress fibers under mechanical stress from periodic stretching." Exp Cell Res **268**(1): 104-14.

Hill, M. A., H. Zou, et al. (2001). "Invited review: arteriolar smooth muscle mechanotransduction: Ca(2+) signaling pathways underlying myogenic reactivity." J Appl Physiol **91**(2): 973-83.

Hollopeter, G., H. M. Jantzen, et al. (2001). "Identification of the platelet ADP receptor targeted by antithrombotic drugs." Nature **409**(6817): 202-7.

Hu, J. and G. R. Lewin (2006). "Mechanosensitive currents in the neurites of cultured mouse sensory neurones." J Physiol **577**(Pt 3): 815-28.

Huang, M. and M. Chalfie (1994). "Gene interactions affecting mechanosensory transduction in Caenorhabditis elegans." Nature **367**(6462): 467-70.

Hynes, M. R. and B. R. Duling (1991). "Ca2+ sensitivity of isolated arterioles from the hamster cheek pouch." Am J Physiol **260**(2 Pt 2): H355-61.

Joe, P., L. D. Wallen, et al. (1997). "Effects of mechanical factors on growth and maturation of the lung in fetal sheep." Am J Physiol **272**(1 Pt 1): L95-105.

Jordt, S. E., D. M. Bautista, et al. (2004). "Mustard oils and cannabinoids excite sensory nerve fibres through the TRP channel ANKTM1." Nature **427**(6971): 260-5.

Katsumi, A., A. W. Orr, et al. (2004). "Integrins in mechanotransduction." J Biol Chem **279**(13): 12001-4.

Kirber, M. T., A. Guerrero-Hernandez, et al. (2000). "Multiple pathways responsible for the stretch-induced increase in Ca2+ concentration in toad stomach smooth muscle cells." J Physiol **524 Pt 1**: 3-17.

Klein, R., I. Silos-Santiago, et al. (1994). "Disruption of the neurotrophin-3 receptor gene trkC eliminates la muscle afferents and results in abnormal movements." Nature **368**(6468): 249-51.

Kolpakov, V., M. D. Rekhter, et al. (1995). "Effect of mechanical forces on growth and matrix protein synthesis in the in vitro pulmonary artery. Analysis of the role of individual cell types." Circ Res **77**(4): 823-31.

Koltzenburg, M., C. L. Stucky, et al. (1997). "Receptive properties of mouse sensory neurons innervating hairy skin." J Neurophysiol **78**(4): 1841-50.

Koo, J. Y., Y. Jang, et al. (2007). "Hydroxy-alpha-sanshool activates TRPV1 and TRPA1 in sensory neurons." Eur J Neurosci **26**(5): 1139-47.

Langton, P. D. (1993). "Calcium channel currents recorded from isolated myocytes of rat basilar artery are stretch sensitive." J Physiol **471**: 1-11.

Li, Y. S., J. H. Haga, et al. (2005). "Molecular basis of the effects of shear stress on vascular endothelial cells." J Biomech **38**(10): 1949-71.

Lumpkin, E. A. and D. M. Bautista (2005). "Feeling the pressure in mammalian somatosensation." Curr Opin Neurobiol **15**(4): 382-8.

Lyford, G. L., P. R. Strege, et al. (2002). "alpha(1C) (Ca(V)1.2) L-type calcium channel mediates mechanosensitive calcium regulation." Am J Physiol Cell Physiol **283**(3): C1001-8.

Maingret, F., M. Fosset, et al. (1999). "TRAAK is a mammalian neuronal mechano-gated K+ channel." J Biol Chem **274**(3): 1381-7.

Maroto, R., A. Raso, et al. (2005). "TRPC1 forms the stretch-activated cation channel in vertebrate cells." Nat Cell Biol **7**(2): 179-85.

McCarron, J. G., C. A. Crichton, et al. (1997). "Myogenic contraction by modulation of voltage-dependent calcium currents in isolated rat cerebral arteries." J Physiol **498 (Pt 2)**: 371-9.

McCarter, G. C., D. B. Reichling, et al. (1999). "Mechanical transduction by rat dorsal root ganglion neurons in vitro." Neurosci Lett **273**(3): 179-82.

McKemy, D. D., W. M. Neuhausser, et al. (2002). "Identification of a cold receptor reveals a general role for TRP channels in thermosensation." Nature **416**(6876): 52-8.

Meyers, J. R., R. B. MacDonald, et al. (2003). "Lighting up the senses: FM1-43 loading of sensory cells through nonselective ion channels." J Neurosci **23**(10): 4054-65.

Mikuni-Takagaki, Y. (1999). "Mechanical responses and signal transduction pathways in stretched osteocytes." J Bone Miner Metab **17**(1): 57-60.

Mizuno, A., N. Matsumoto, et al. (2003). "Impaired osmotic sensation in mice lacking TRPV4." Am J Physiol Cell Physiol **285**(1): C96-101.

Muraki, K., Y. Iwata, et al. (2003). "TRPV2 is a component of osmotically sensitive cation channels in murine aortic myocytes." Circ Res **93**(9): 829-38.

O'Hagan, R., M. Chalfie, et al. (2005). "The MEC-4 DEG/ENaC channel of Caenorhabditis elegans touch receptor neurons transduces mechanical signals." Nat Neurosci **8**(1): 43-50.

Page, A. J., S. M. Brierley, et al. (2004). "The ion channel ASIC1 contributes to visceral but not cutaneous mechanoreceptor function." Gastroenterology **127**(6): 1739-47.

Pasantes-Morales, H., R. A. Lezama, et al. (2006). "Mechanisms of cell volume regulation in hypo-osmolality." Am J Med **119**(7 Suppl 1): S4-11.

Prescott, E. D. and D. Julius (2003). "A modular PIP2 binding site as a determinant of capsaicin receptor sensitivity." Science **300**(5623): 1284-8.

Price, M. P., G. R. Lewin, et al. (2000). "The mammalian sodium channel BNC1 is required for normal touch sensation." Nature **407**(6807): 1007-11.

Price, M. P., S. L. McIlwrath, et al. (2001). "The DRASIC cation channel contributes to the detection of cutaneous touch and acid stimuli in mice." Neuron **32**(6): 1071-83.

Ramsey, I. S., M. Delling, et al. (2006). "An introduction to TRP channels." Annu Rev Physiol **68**: 619-47.

Ross, R. (1993). "The pathogenesis of atherosclerosis: a perspective for the 1990s." Nature **362**(6423): 801-9.

Roza, C., J. L. Puel, et al. (2004). "Knockout of the ASIC2 channel in mice does not impair cutaneous mechanosensation, visceral mechanonociception and hearing." J Physiol **558**(Pt 2): 659-69.

Russell, F. E., C. B. Alender, et al. (1968). "Venom of the Scorpion Vejovis spinigerus." Science **159**(3810): 90-91.

Schwartz, E. F., C. A. Schwartz, et al. (2006). "HgeTx1, the first K+-channel specific toxin characterized from the venom of the scorpion Hadrurus gertschi Soleglad." Toxicon **48**(8): 1046-53.

Sidi, S., R. W. Friedrich, et al. (2003). "NompC TRP channel required for vertebrate sensory hair cell mechanotransduction." Science **301**(5629): 96-9.

Siemens, J., S. Zhou, et al. (2006). "Spider toxins activate the capsaicin receptor to produce inflammatory pain." Nature **444**(7116): 208-12.

Strotmann, R., C. Harteneck, et al. (2000). "OTRPC4, a nonselective cation channel that confers sensitivity to extracellular osmolarity." Nat Cell Biol **2**(10): 695-702.

Stucky, C. L., K. A. Medler, et al. (2004). "The P2Y agonist UTP activates cutaneous afferent fibers." Pain **109**(1-2): 36-44.

Suchyna, T. M., J. H. Johnson, et al. (2000). "Identification of a peptide toxin from Grammostola spatulata spider venom that blocks cation-selective stretch-activated channels." J Gen Physiol **115**(5): 583-98.

Suchyna, T. M., S. E. Tape, et al. (2004). "Bilayer-dependent inhibition of mechanosensitive channels by neuroactive peptide enantiomers." Nature **430**(6996): 235-40.

Sukharev, S. I., P. Blount, et al. (1994). "A large-conductance mechanosensitive channel in E. coli encoded by mscL alone." Nature **368**(6468): 265-8.

Suzuki, M., A. Mizuno, et al. (2003). "Impaired pressure sensation in mice lacking TRPV4." J Biol Chem **278**(25): 22664-8.

Takahashi, A. and H. Gotoh (2000). "Mechanosensitive whole-cell currents in cultured rat somatosensory neurons." Brain Res **869**(1-2): 225-30.

Vellani, V., S. Mapplebeck, et al. (2001). "Protein kinase C activation potentiates gating of the vanilloid receptor VR1 by capsaicin, protons, heat and anandamide." J Physiol **534**(Pt 3): 813-25.

Viana, F., E. de la Pena, et al. (2001). "Swelling-activated calcium signalling in cultured mouse primary sensory neurons." Eur J Neurosci **13**(4): 722-34.

Vlaskovska, M., L. Kasakov, et al. (2001). "P2X3 knock-out mice reveal a major sensory role for urothelially released ATP." J Neurosci **21**(15): 5670-7.

Waitkus-Edwards, K. R., L. A. Martinez-Lemus, et al. (2002). "alpha(4)beta(1) Integrin activation of L-type calcium channels in vascular smooth muscle causes arteriole vasoconstriction." Circ Res **90**(4): 473-80.

Walker, R. G., A. T. Willingham, et al. (2000). "A Drosophila mechanosensory transduction channel." Science **287**(5461): 2229-34.

Waters, C. M., P. H. Sporn, et al. (2002). "Cellular biomechanics in the lung." Am J Physiol Lung Cell Mol Physiol **283**(3): L503-9.

Waxman, S. G., S. Dib-Hajj, et al. (1999). "Sodium channels and pain." Proc Natl Acad Sci U S A **96**(14): 7635-9.

Wetzel, C., J. Hu, et al. (2007). "A stomatin-domain protein essential for touch sensation in the mouse." Nature **445**(7124): 206-9.

Wu, X., G. E. Davis, et al. (2001). "Regulation of the L-type calcium channel by alpha 5beta 1 integrin requires signaling between focal adhesion proteins." J Biol Chem **276**(32): 30285-92.

Wu, X. and M. J. Davis (2001). "Characterization of stretch-activated cation current in coronary smooth muscle cells." Am J Physiol Heart Circ Physiol **280**(4): H1751-61.

Wu, X., J. E. Mogford, et al. (1998). "Modulation of calcium current in arteriolar smooth muscle by alphav beta3 and alpha5 beta1 integrin ligands." J Cell Biol **143**(1): 241-52.

Xu, L., A. Tripathy, et al. (1999). "Ruthenium red modifies the cardiac and skeletal muscle Ca(2+) release channels (ryanodine receptors) by multiple mechanisms." J Biol Chem **274**(46): 32680-91.

Zou, H., L. M. Lifshitz, et al. (2002). "Visualization of Ca2+ entry through single stretch-activated cation channels." Proc Natl Acad Sci U S A **99**(9): 6404-9.

Publishing Agreement

It is the policy of the University to encourage the distribution of all theses and dissertations. Copies of all UCSF theses and dissertations will be routed to the library via the Graduate Division. The library will make all theses and dissertations accessible to the public and will preserve these to the best of their abilities, in perpetuity.

I hereby grant permission to the Graduate Division of the University of California, San Francisco to release copies of my thesis or dissertation to the Campus Library to provide access and preservation, on whole or in part, in perpetuity.

Martha Ruth Chase — Author Signature

11/26/07 — Date